ALZHEIMER'S DISEASE

Amyloid-β peptide protects against microbial infection in mouse and worm models of Alzheimer's disease

Deepak Kumar Vijaya Kumar,[1]* Se Hoon Choi,[1]* Kevin J. Washicosky,[1]* William A. Eimer,[1] Stephanie Tucker,[1] Jessica Ghofrani,[1] Aaron Lefkowitz,[1] Gawain McColl,[2] Lee E. Goldstein,[3] Rudolph E. Tanzi,[1†] Robert D. Moir[1†]

The amyloid-β peptide (Aβ) is a key protein in Alzheimer's disease (AD) pathology. We previously reported in vitro evidence suggesting that Aβ is an antimicrobial peptide. We present in vivo data showing that Aβ expression protects against fungal and bacterial infections in mouse, nematode, and cell culture models of AD. We show that Aβ oligomerization, a behavior traditionally viewed as intrinsically pathological, may be necessary for the antimicrobial activities of the peptide. Collectively, our data are consistent with a model in which soluble Aβ oligomers first bind to microbial cell wall carbohydrates via a heparin-binding domain. Developing protofibrils inhibited pathogen adhesion to host cells. Propagating β-amyloid fibrils mediate agglutination and eventual entrapment of unatttached microbes. Consistent with our model, *Salmonella* Typhimurium bacterial infection of the brains of transgenic 5XFAD mice resulted in rapid seeding and accelerated β-amyloid deposition, which closely colocalized with the invading bacteria. Our findings raise the intriguing possibility that β-amyloid may play a protective role in innate immunity and infectious or sterile inflammatory stimuli may drive amyloidosis. These data suggest a dual protective/damaging role for Aβ, as has been described for other antimicrobial peptides.

INTRODUCTION

Neurodegeneration in Alzheimer's disease (AD) is mediated by soluble oligomeric intermediates generated during fibrillization of the amyloid-β protein (Aβ) (*1*). Overwhelming evidence supports Aβ's pivotal role in AD. However, despite remarkably high sequence conservation across diverse species (humans share Aβ42 sequences with coelacanths, a 400 million–year–old fish taxon) (*2*) and extensive data showing broad activity spectra for Aβ, the peptide has traditionally been characterized as a functionless catabolic byproduct. Activities identified for Aβ in vivo are most often described as stochastic pathological behaviors. Oligomerization, in particular, is viewed as a pathogenic pathway, and Aβ oligomers are assumed to be intrinsically abnormal. Scant consideration has been given to possible physiological roles for Aβ.

Members of the evolutionarily ancient family of proteins, collectively known as antimicrobial peptides (AMPs), share many of Aβ's purportedly abnormal activities, including oligomerization and fibrillization (*3*, *4*). For AMPs, these activities mediate key protective roles in innate immunity. AMPs are the first line of defense against pathogens and act as potent broad-spectrum antibiotics and immunomodulators that target bacteria, mycobacteria, enveloped viruses, fungi, protozoans, and, in some cases, transformed or cancerous host cells (*5*). AMPs are widely expressed and are abundant in brain and other immunoprivileged tissues where actions of the adaptive immune system are constrained. Although AMPs are normally protective, AMP dysregulation can lead to host cell toxicity, chronic inflammation, and degenerative pathologies (*6*–*8*). Particularly germane to Aβ's role in AD, AMPs are deposited as amyloid in several disorders (*3*, *4*, *9*), including senile seminal vesicle amyloid and isolated atrial amyloidosis, two of the most common human amyloidopathies. Consistent with identity as an AMP, we recently reported that synthetic Aβ exhibits potent in vitro antimicrobial activity toward eight common and clinically relevant microbial pathogens (*3*). Furthermore, whole-brain homogenates from AD patients show Aβ-mediated activity against *Candida albicans*. More recently, synthetic Aβ has been shown to protect cultured cells from influenza A virus (*10*) and herpes simplex virus (*11*). However, the biological relevance of protective in vitro Aβ activities requires validation in vivo. Here, we extend our original findings and show that Aβ expression inhibits infection in a transgenic mouse model of AD (5XFAD), in the nematode *Caenorhabditis elegans*, and in cultured mammalian cell models. Mice lacking the amyloid precursor protein (APP) that have low Aβ expression also show a trend toward attenuated survival after bacterial infection. Most surprisingly, oligomerization and fibrillization appear to mediate Aβ's protective activity, and cerebral infection with microbial cells seeds and markedly accelerates β-amyloid deposition in 5XFAD mice and transgenic *C. elegans*.

RESULTS

Aβ-mediated protection was characterized in mice, *C. elegans*, and cell culture models of infection. *Salmonella enterica* serotype Typhimurium (*S.* Typhimurium) was used as an infecting agent in mouse models. Nematode and cultured cell experiments used pathogenic (hyphal) *C. albicans* (*Candida*) and *S.* Typhimurium.

Aβ protects against meningitis in genetically modified mice

We first used genetically modified mice to test for protective effects of elevated Aβ expression and attenuated resistance with decreased peptide. Four-week-old 5XFAD transgenic mice constitutively express human Aβ in the brain at high levels but lack the β-amyloid deposits and features

[1]Genetics and Aging Research Unit, MassGeneral Institute for Neurodegenerative Disease, Department of Neurology, Massachusetts General Hospital and Harvard Medical School, Charlestown, MA 02129, USA. [2]The Florey Institute of Neuroscience and Mental Health, University of Melbourne, Parkville, Victoria 3052, Australia. [3]Department of Psychiatry, Boston University, Boston, MA 02215, USA.
*These authors contributed equally to this work.
†Corresponding author. Email: moir@helix.mgh.harvard.edu (R.D.M.); tanzi@helix.mgh.harvard.edu (R.E.T.)

of neuroinflammation found in older animals (*12*). APP knockout (APP-KO) mice lack the precursor protein required for murine Aβ generation (*13*). One-month-old 5XFAD mice (n = 12), APP-KO mice (n = 15), and wild-type littermates (n = 11 and 15, respectively) received a single intracerebral injection of 65,000 colony-forming units (CFU) of *S.* Typhimurium. Clinical progression to the moribund state was followed according to established grading criteria for mouse encephalomyelitis (fig. S1A). Survival of Aβ-expressing 5XFAD mice was significantly increased compared to that of nontransgenic littermates (P = 0.009) (Fig. 1A). Consistent with increased resistance to infection, 5XFAD mice also ranked significantly higher in clinical tests grading mouse encephalomyelitis progression (P < 0.0001). 5XFAD mice also showed reduced weight loss (P = 0.0008) and lower cerebral *S.* Typhimurium loads (P = 0.03) compared to wild-type controls (Fig. 1, B to D). Consistent with immunodeficiency associated with low Aβ, APP-KO mice showed a trend (P = 0.10) toward increased mortality after infection (Fig. 1E). Control injections using heat-killed bacteria did not lead to clinical decline or death in 5XFAD and wild-type mice (Fig. 1F), consistent with mouse mortality being mediated by *S.* Typhimurium infection. Next, we confirmed high amounts of soluble Aβ and low amounts of insoluble Aβ in 4-week-old 5XFAD mouse brain using formic acid extraction and anti–β-amyloid enzyme-linked immunosorbent assays (ELISAs) (fig. S1B). To confirm that inflammation did not immunologically prime and protect 5XFAD mice against infection, we compared the immune profiles in 1-month-old transgenic and wild-type mouse brains. Consistent with previous reports showing an absence of immune activation (*12*), there was no significant increase in glial fibrillary acidic protein–positive ($GFAP^+$) astrocytes, $lba1^+$ microglia, and the amounts of 10 cytokines in 4-week-old 5XFAD mice compared to wild-type littermates (fig. S1, C to E).

Aβ increases survival of transgenic *C. elegans* infected with *Candida*

To further explore the ability of Aβ to afford protection against infection, we next tested transgenic *C. elegans* for resistance to *Candida*. Our nematode infection model uses two previously described *C. elegans* transgenic strains: GMC101 that expresses the 1–42 residue human Aβ isoform (Aβ42) (*14*) and CL2122, a control strain that expresses intestinal green fluorescent protein (GFP) (*mtl-2:gfp*) marker (as does GMC101) but does not express Aβ. Adult GMC101 nematodes ultimately develop age-progressive paralysis and β-amyloid deposition in the body wall muscle. For our experiments, developmentally synchronized L4 larvae were infected 5 days before the onset of paralysis. Aβ expression is driven by the *unc-54* promoter (which encodes a myosin heavy chain), active in body wall muscle (*14*) as well as in other tissues, including muscle cells of the gastrointestinal tract (*15*). Amyloidogenic peptides under the *unc-54* promoter have also been shown to translocate via vesicular transport to the gut of transgenic worms, and Aβ has been proposed as a likely candidate for translocation via this mechanism (*16*). Immunohistological analysis of adult GMC101 using three different anti-Aβ antibodies confirmed Aβ localization in the body wall muscle and the gut lumen (fig. S2, A and B). Anti-Aβ antibodies did not label negative control strain CL2122 intestine or body wall cells. In addition, excreta from healthy GMC101 but not CL2122 worms were positive for anti-Aβ signal by immunoblot (fig. S2C). Although an origin for gut Aβ remains unclear, strong empirical evidence supports the localization of Aβ peptides in the intestinal lumen of GMC101 nematodes. Thus, transgenic GMC101 nematodes appear to be suitable models for testing Aβ-mediated protective activities against intestinal pathogens.

C. albicans [American Type Culture Collection (ATCC) 90028] is an Aβ-sensitive

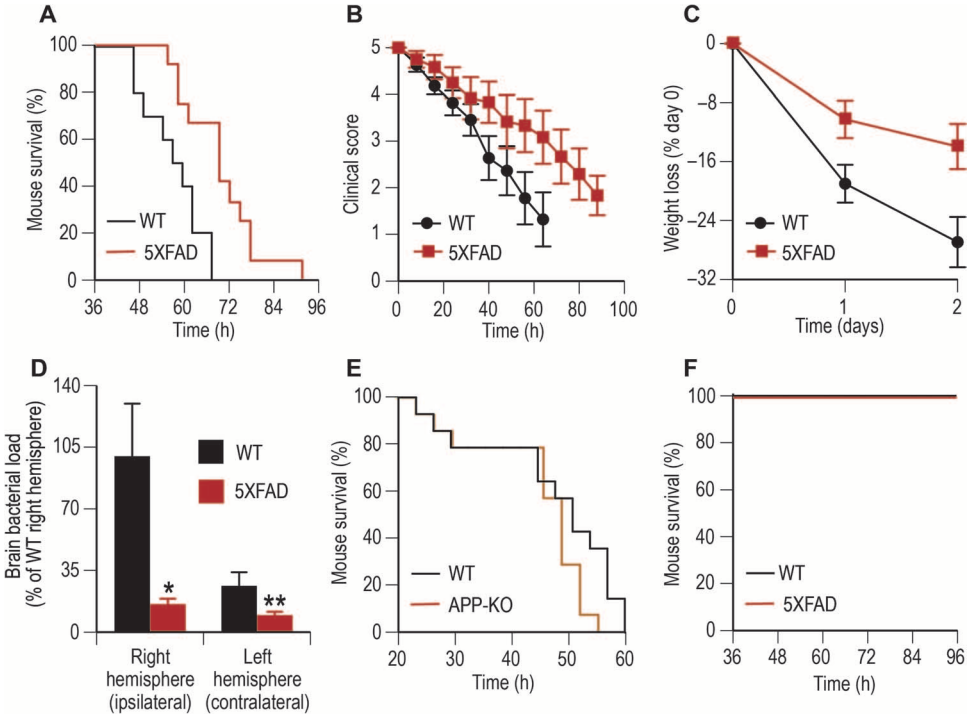

Fig. 1. Aβ expression protects against *S.* Typhimurium meningitis in genetically modified AD mouse models. Transgenic (5XFAD) mice expressing human Aβ and mice lacking murine APP (APP-KO) were compared to genetically unmodified littermates [wild type (WT)] for resistance to *S.* Typhimurium meningitis. One-month-old mice received single ipsilateral intracranial injections of *S.* Typhimurium, and clinical progression was followed to moribundity. (**A** to **C**) Performance of 5XFAD (n = 12) mice compared to WT (n = 11) are shown after infection for survival (P = 0.009) (A), clinical score (P < 0.0001) (B), and percent weight loss (P = 0.0008) (C). (**D**) *S.* Typhimurium load 24 hours after infection in 5XFAD (n = 4) and WT (n = 4) mouse brain hemisphere homogenates shown as mean CFU ± SEM (*P = 0.03 and **P = 0.04). (**E**) APP-KO mice (n = 15) show a trend (P = 0.104) toward reduced survival compared to WT (n = 15) littermates after infection. (**F**) No mortality was observed among control sham-infected WT (n = 6) or 5XFAD (n = 6) mice injected with heat-killed *S.* Typhimurium. Statistical significance was calculated by log-rank (Mantel-Cox) test for survival (A, E, and F), linear regression for clinical score and weight (B and C), and statistical means compared by t test for brain bacterial loads (D). For survival and clinical analysis (A to C), data were pooled from three independent experiments.

dimorphic fungus (*3*) and a well-characterized *C. elegans* intestinal pathogen that causes distention, penetrative filamentation, and death among wild-type nematodes 2 days after ingestion. Links between fungal brain infections and AD pathology have also recently emerged, including for *C. albicans* (*17*) and closely related *Candida glabrata* (*18*). We compared survival of control CL2122 ($n = 56$) and GMC101 ($n = 59$) nematodes after incubation (2 hours, 25°C) on *C. albicans* lawns. Consistent with Aβ-mediated protection, GMC101 nematodes infected with *C. albicans* showed significantly ($P < 0.00001$) reduced mortality as compared to control CL2122 worms that did not express Aβ (Fig. 2A). Consistent with mouse data, Aβ-expressing nematodes were also protected from the *C. elegans* intestinal pathogen *S.* Typhimurium with GMC101 worms showing statistically significant ($P = 0.0005$) increased survival compared to CL2122 controls after infection with the bacterium (fig. S3A).

The antimicrobial activities of Aβ protects cells in culture

To address the mechanism of protection, we next tested the ability of Aβ to protect cell monolayers from infection using transformed cultured human brain neuroglioma (H4) and Chinese hamster ovary (CHO) cells. H4 lines included stably transformed H4-Aβ40 and H4-Aβ42 cells that selectively secrete the 1–40 residue Aβ isoform (Aβ40) or Aβ42 isoform, respectively (*19*). Processing of a BRI-Aβ fusion protein expressed by transformed H4 cells led to constitutive high-level expression and secretion of the encoded Aβ protein. For double transfected CHO cells (CHO-CAB), overexpression of APP and the APP-processing protease β-secretase leads to APP cleavage and the generation of multiple Aβ isoforms (*20*). Non-transformed H4 (H4-N) and CHO (CHO-N) cells were used as control cell lines. *C. albicans* has been extensively characterized

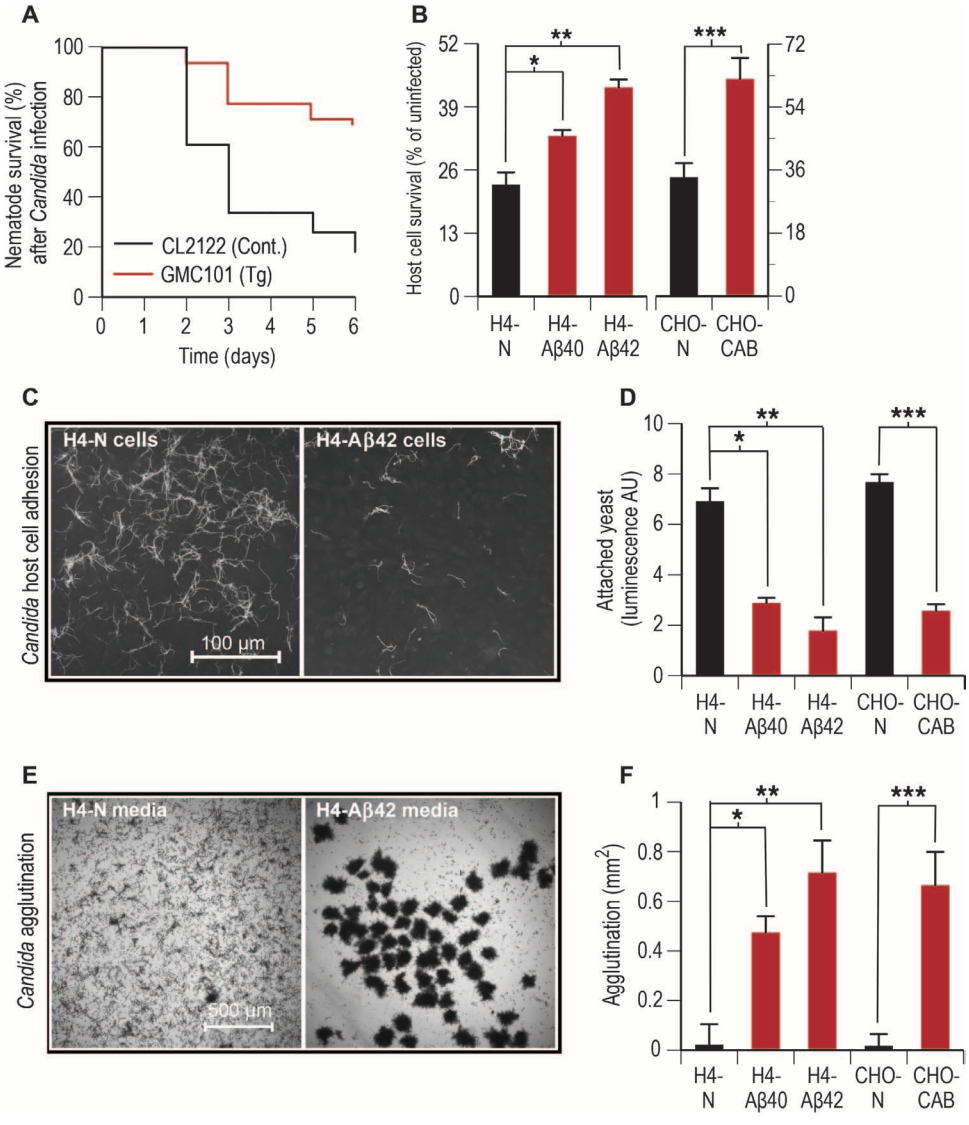

Fig. 2. Aβ expression in nematodes and cultured cells increases host resistance to infection by *Candida*. Aβ-mediated protection against *C. albicans* (*Candida*) was characterized in *C. elegans* and cultured host cell monolayer mycosis models. Experimental nematodes included control (Cont.) non-Aβ expressing (CL2122) and transgenic (Tg) human Aβ-expressing (GMC101) strains. Host cell lines included control nontransformed (H4-N and CHO-N) and transformed Aβ-overexpressing (H4-Aβ40, H4-Aβ42, and CHO-CAB) cells. (**A**) Survival curves for CL2122 ($n = 61$) and GMC101 ($n = 57$) nematodes after infection with *Candida* ($P < 0.00001$). (**B**) Viability of nontransformed and transformed host cell monolayers after 28-hour incubation with *Candida*. Host cell viability was followed by prelabeling host cell monolayers with BrdU and then comparing wells for an anti-BrdU signal. Signal of infected wells shown as percentage of uninfected control wells (*$P = 0.002$, **$P = 0.001$, and ***$P = 0.004$). (**C**) *Candida* adherence to host cells. Fluorescence micrograph of Calcofluor white–stained *Candida* adhering to control H4-N or transformed H4-Aβ42 host cell monolayers after 2 hours of co-incubation in preconditioned culture medium. (**D**) Quantitative analysis of *Candida* host cell colonization. Adhering *Candida* were detected using an immunochemical luminescence assay with anti-*Candida* antibodies (*$P = 0.003$, **$P = 0.001$, and ***$P = 0.004$). Well comparisons use arbitrary luminescence units (AU). (**E**) Phase-contrast micrographs of agglutinated *Candida* after overnight incubation with H4-N or H4-Aβ42 host cells. (**F**) Quantitative analysis of *Candida* agglutination. Wells were compared for yeast aggregate surface area using image analysis software (*$P = 0.007$, **$P = 0.002$, and ***$P = 0.009$). Bars in (B), (D), and (F) are means of six replicate wells ± SEM. Statistical significance was calculated by log-rank (Mantel-Cox) test for nematode survival (A) and statistical mean comparisons by *t* test (B, D, and F). Micrographs (C and E) are representative of data from three replicate experiments and multiple discrete image fields (table S1A).

in cell culture infection models and was used in our experiments as an infectious agent.

We first compared nontransformed and transformed host cells for survival after infection with *C. albicans*. Host cells were prelabeled with bromodeoxyuridine (BrdU). After infection, host cell viability was determined by assaying for anti-BrdU immunofluorescence. Consistent with findings for 5XFAD mice and GMC101 nematodes, survival 28 hours after infection was significantly increased for Aβ-overexpressing H4-Aβ40 ($P = 0.002$) and H4-Aβ42 ($P = 0.001$) transformed cell lines compared to control H4-N cells, with rank order H4-Aβ42 > H4-Aβ40 > H4-N (Fig. 2B). Survival of transformed CHO-CAB cells was also significantly higher ($P = 0.004$) than that of control CHO-N cell lines. Additional independent assays of host cell viability (fig. S4, A and B) were performed to confirm increased resistance of transformed H4-Aβ42 cells to *C. albicans* infection. Attenuated *C. albicans* load for H4-Aβ42 cells was also independently confirmed by comparing wells for yeast CFU (fig. S4C).

Whereas the amount of Aβ in conditioned cell culture medium (fig. S5, A and B) fell within the physiological ranges reported for human cerebrospinal fluid (CSF) (2 to 20 ng/ml) (*21*), concentrations were two orders of magnitude ($\log_{10}$) lower than the minimal inhibitory concentration (MIC) for fungicidal activities in microdilution MIC assays (*3*). We have previously reported that Aβ's antimicrobial activities show close parallels with those of LL-37 (*3*), an archetypal human AMP that remains protective at subfungicidal concentrations (*22*). Two linked, yet distinct activities mediate LL-37's protective anti-*Candida* actions at low peptide concentrations (*22*). The first is disruption of *C. albicans* adhesion to host cells. Host cell attachment is a prerequisite step for infection by many pathogens, including *C. albicans*. The second is agglutination of the resulting unattached yeast cells. Agglutination limits microbial access to host cells and also generates high local AMP concentrations within peptide/microbe aggregates. Accordingly, we next tested Aβ for adhesion inhibition and agglutination activities using the cell culture infection model. Hyphal *C. albicans* was incubated (2 hours, 37°C) in preconditioned medium with transformed or nontransformed cell cultures prepared in slide chambers. Microscopic examination revealed fewer *C. albicans* attached to transformed Aβ-expressing cells compared to nontransformed monolayers (Fig. 2C and fig. S6A). To confirm these data, we repeated *C. albicans*–cell culture incubation experiments in 96-well microtiter plates, and we assayed the *Candida* load in wells immunochemically using anti-*Candida* antibodies. Data confirmed visual observations with statistically significant attenuation of *C. albicans* adhesion to transformed H4-Aβ42 ($P = 0.001$), H4-Aβ40 ($P = 0.001$), and CHO-CAB ($P = 0.004$) cells compared to naive control lines (Fig. 2D). Additionally, after overnight incubation, marked microbial agglutination was observed in wells containing transformed, but not nontransformed, host cells (Fig. 2E and fig. S6B). Images of wells were analyzed for yeast aggregation. *Candida* aggregation was significantly elevated in transformed H4-Aβ42 ($P = 0.00004$), H4-Aβ40 ($P = 0.0003$), and CHO-CAB ($P = 0.002$) samples compared to naive controls (Fig. 2F). For H4 cell lines, adhesion inhibition and agglutination activities were consistent with host viability data, with rank orders H4-Aβ42 > H4-Aβ40 > H4-N.

We next characterized cell-free conditioned culture medium for Aβ-mediated adhesion inhibition and agglutinating activities. Yeast adhesion and agglutination were assayed in 96-well plates using the methods of Tsai *et al.* (*22*). Briefly, synchronized hyphal *C. albicans* were incubated (2 hours, 37°C) with conditioned medium samples in the absence of host cells. After washing, yeast adhering to well surfaces were stained with Calcofluor white, and fluorescence was measured. Well images were analyzed for yeast aggregation after overnight incubation. Immunodepletion with anti-Aβ antibodies significantly attenuated H4-Aβ42, H4-Aβ40, and CHO-CAB medium adhesion inhibition ($P = 0.009$, $P = 0.001$, and $P = 0.004$, respectively) and agglutination ($P = 0.001$, $P = 0.0005$, and $P = 0.004$, respectively) activities against *C. albicans* (Fig. 3, A and B). Analysis confirmed that anti-Aβ immunodepletion removed >95% of the Aβ from samples used in experiments to confirm that the anti-*Candida* activities of transformed cell culture medium were specific for Aβ (fig. S5, A and B).

Consistent with yeast data, *S.* Typhimurium were agglutinated in H4-Aβ42 conditioned medium (fig. S3B). H4-Aβ42 cell cultures incubated with *S.* Typhimurium also have significantly ($P = 0.036$) lower intracellular infection compared to nontransformed H4-N cells (fig. S3, C and D).

Serial dilution experiments showed that adhesion inhibition and agglutination activities were dose-dependent for both synthetic and cell-derived Aβ (Fig. 3, C and D). However, synthetic Aβ peptide preparations had lower specific activities compared to cell-derived material. Cofactors secreted by cultured cells were unlikely to account for the increased potency of cell-derived Aβ because synthetic peptide incubations were performed in Aβ42-depleted conditioned medium (H4-Aβ42-ID) from H4-Aβ42 cell cultures. Anti-Aβ antibodies used to clear Aβ42 from H4-Aβ42 culture medium before addition of synthetic peptides were specific for Aβ and not likely to deplete species acting as cofactors. Oligomerization has been shown to modulate a range of Aβ activities. Moreover, conditioned medium from experimental cell lines has been reported to contain oligomeric Aβ (*23*), whereas our synthetic peptide preparations were pretreated to remove oligomer species. Synthetic peptide pretreatments included fractionation by preparative size exclusion chromatography to remove species >6 kD. Characterization experiments using analytical size exclusion chromatography confirmed that immediately before experimental inoculation with yeast, cell-derived material contained a polydisperse population of soluble Aβ oligomers of between 8 and 50 kD, whereas synthetic peptides remained overwhelmingly monomeric (fig. S5C).

To test whether oligomerization modulates Aβ's AMP activity, we generated synthetic Aβ oligomers and compared the antimicrobial activities of Aβ42 monomer, soluble oligomeric ADDLs (amyloid-β–derived diffusible oligomeric ligands) (*24*), and high-order protofibril (>600 kD) preparations. Compared to monomeric peptide, ADDLs exhibited potentiated, and protofibrils attenuated, adhesion inhibition (Fig. 3E) and agglutination (Fig. 3F) activities. Our data are consistent with a central role for soluble Aβ low-order (2 to 30 monomer units) oligomers in mediating the peptide's AMP activities. Consistent with such a role, soluble Aβ is overwhelmingly oligomeric in vivo (*25*), and oligomers are key for the protective activities of a wide range of AMPs (*26*–*29*) including LL-37 (*26*, *30*).

Antimicrobial actions are mediated by the heparin-binding activity of Aβ oligomers

Binding of AMP peptides to microbial surfaces is a prerequisite step for adhesion inhibition and agglutination activities. LL-37 contains an XBBXBX heparin-binding motif (where X is a hydrophobic or uncharged residue and B is a basic residue) that mediates inhibition of host cell adhesion and agglutination activities by facilitating attachment of

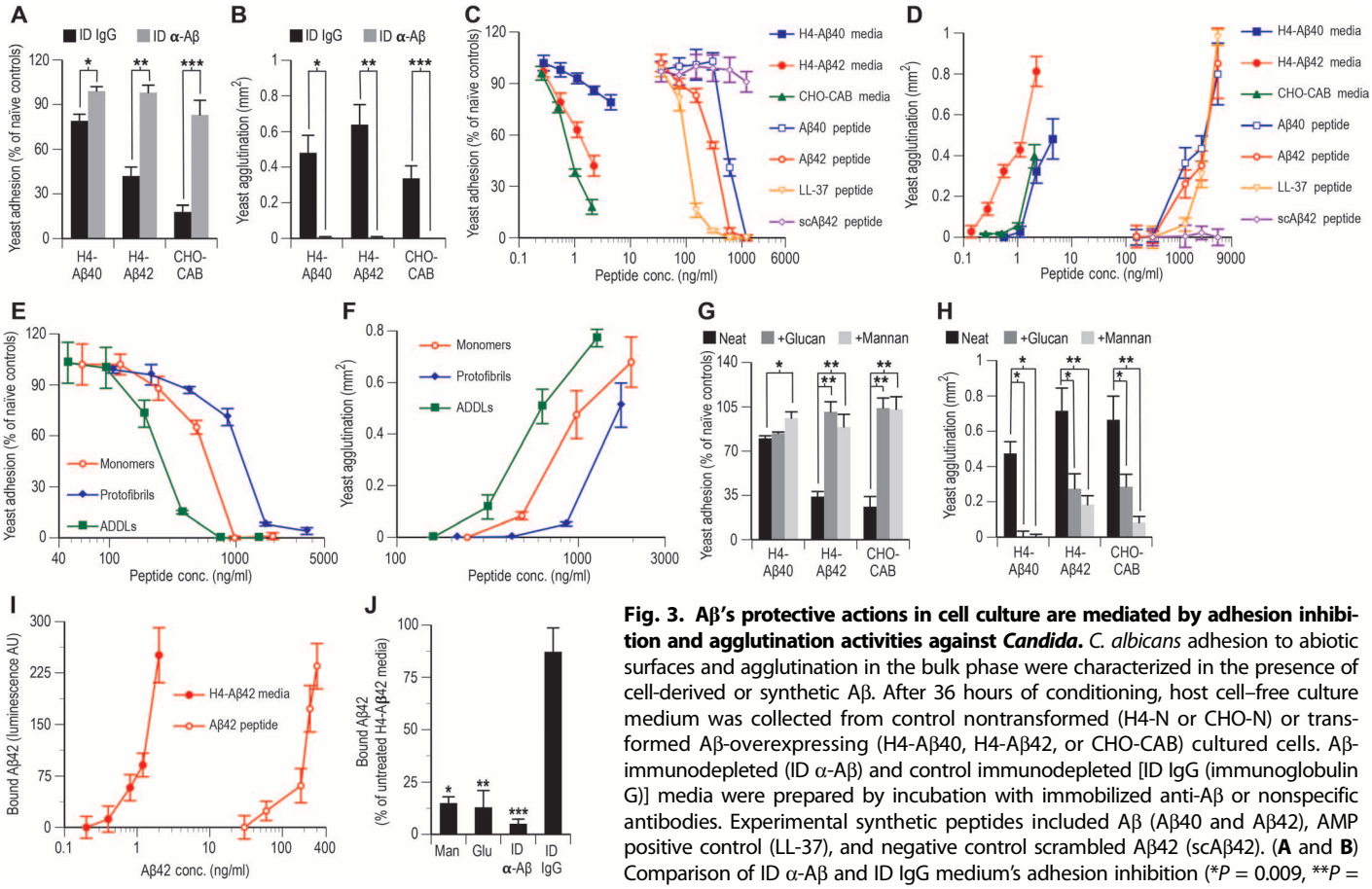

Fig. 3. Aβ's protective actions in cell culture are mediated by adhesion inhibition and agglutination activities against *Candida*. *C. albicans* adhesion to abiotic surfaces and agglutination in the bulk phase were characterized in the presence of cell-derived or synthetic Aβ. After 36 hours of conditioning, host cell–free culture medium was collected from control nontransformed (H4-N or CHO-N) or transformed Aβ-overexpressing (H4-Aβ40, H4-Aβ42, or CHO-CAB) cultured cells. Aβ-immunodepleted (ID α-Aβ) and control immunodepleted [ID IgG (immunoglobulin G)] media were prepared by incubation with immobilized anti-Aβ or nonspecific antibodies. Experimental synthetic peptides included Aβ (Aβ40 and Aβ42), AMP positive control (LL-37), and negative control scrambled Aβ42 (scAβ42). (**A** and **B**) Comparison of ID α-Aβ and ID IgG medium's adhesion inhibition (*P = 0.009, **P = 0.001, and ***P = 0.004) and agglutination (*P = 0.001, **P = 0.0005, and ***P = 0.004) activities. (**C** and **D**) Comparison of anti-*Candida* activities of serially diluted conditioned medium and synthetic peptides. (**E** and **F**) Activities of synthetic Aβ42 monomer, soluble oligomeric ADDLs, and protofibril preparations. (**G** and **H**) Conditioned culture medium adhesion inhibition (*P = 0.003 and **P < 0.0003) and agglutinating (*P < 0.02 and **P < 0.003) source activities alone (Neat) or in the presence of soluble yeast wall carbohydrates (+Glucan or +Mannan). (**I**) Synthetic monomeric Aβ42 and cell-generated peptide from H4-Aβ42 cells were compared for *Candida* binding using an Aβ/*Candida* binding ELISA. (**J**) Untreated, immunodepleted, or glucan (Glu)- or mannan (Man)–spiked H4-Aβ42 conditioned media were incubated with intact immobilized yeast cells in an Aβ/*Candida* binding ELISA assay (*P = 0.006, **P = 0.008, and ***P < 0.004). Synthetic peptide incubations (C to F and I) were performed in H4-Aβ42 conditioned culture medium pretreated to remove cell-derived Aβ by α-Aβ immunodepletion. Symbols and bars for (A) to (J) are statistical means of six replicate wells ± SEM. Statistical significance was by *t* test.

oligomeric species (*26*, *30*) to microbial cell wall carbohydrates (*22*). Aβ also contains an XBBXBX heparin-binding motif between residues 12 to 17 (VHHQKL) (*31*). Competitive inhibition by soluble microbial sugars is a hallmark for AMPs with activities mediated by lectin-like carbohydrate binding (*22*). Indeed, fungal and bacterial pathogens secrete specialized scavenging exopolysaccharides that target the heparin-binding domains of AMPs as a countermeasure to defenses mounted by hosts. Soluble forms of mannan and glucan, the two most abundant carbohydrates in the yeast cell wall, have been shown to inhibit XBBXBX-mediated binding of LL-37 to *Candida* (*22*, *32*). We investigated whether the adhesion inhibition and agglutination activities of Aβ were similarly inhibited by soluble mannan and glucan. Live yeast cells were incubated in H4-Aβ40, H4-Aβ42, and CHO-CAB conditioned medium in the presence or absence of mannan or glucan. Consistent with anti-*Candida* activity mediated by Aβ's heparin-binding domain, mannan and glucan significantly attenuated adhesion inhibition (P < 0.008) and agglutination (P < 0.003) activities of conditioned medium from Aβ-expressing transformed cells (Fig. 3, G and H).

We further characterized Aβ's binding to *C. albicans* and *S.* Typhimurium using a new binding immunoassay. For this assay, samples were incubated in wells containing immobilized intact hyphal *Candida* or *S.* Typhimurium cells, and bound Aβ was detected immunochemically with an Aβ42-specific antibody. Aβ binding to *Candida* and *S.* Typhimurium was concentration-dependent (Fig. 3I and fig. S3E). Consistent with binding mediated by Aβ's VHHQKL domain, the anti-Aβ signal from H4-Aβ42 medium was significantly attenuated in the presence of glucan (P = 0.008) or mannan (P = 0.004) (Fig. 3J). The anti-Aβ signal in wells was also significantly reduced (P = 0.006) for anti-Aβ–immunodepleted H4-Aβ42 medium (negative control), which was consistent with assay specificity for Aβ42 binding. Consistent with findings for antimicrobial activities, cell-generated Aβ oligomers showed increased binding to immobilized yeast compared to synthetic monomeric peptide (Fig. 3I). Previous studies have shown that Aβ oligomerization greatly increases carbohydrate-binding activity (*31*). Heparin-binding AMP oligomers also show potentiated carbohydrate binding compared to monomeric species (*33*). Overall,

our findings are consistent with soluble Aβ oligomers having an enhanced propensity to bind to cell walls, engendering greater adhesion inhibition and agglutination activities compared to monomeric synthetic peptide.

Aβ fibrillization mediates *Candida* agglutination

Binding by Aβ of glycosaminoglycans found in brain tissue induces peptide fibrillization (*34*). Aβ's binding of cell wall and glycocalyx carbohydrates at microbial surfaces seemed likely to also generate Aβ fibrils. Although viewed solely as a part of Aβ's pathophysiology, fibrillization among AMPs is a normal protective behavior that mediates antimicrobial activities, including microbial cell and viral agglutination (*35*) and bacterial membrane perturbation (*3*, *4*). Most recently, studies have shown that the human AMP α-defensin-6 (HD6) forms fibrils that entangle and trap microbial cells (*36*). Thus, we next investigated a possible role for Aβ fibrillization in the peptide's protective AMP activities. Analysis of early-stage (<3 hours after infection) *Candida* agglutination in H4-Aβ42 medium using transmission electron microscopy (TEM) revealed clumped microbial cells entwined and linked by fibrils propagating from cell surfaces (Fig. 4, A to D). *C. albicans* lack flagella and are not reported to produce extended fibrillar structures. Moreover, the fibrillar structures on the *Candida* cell surface were labeled by anti–Aβ immunogold nanoparticles (anti–Aβ-Au). Anti–Aβ-Au binding to fibrils was ablated by co-incubation with synthetic Aβ peptide, consistent with Aβ-specific labeling (Fig. 4D). TEM analysis of early-stage *S.* Typhimurium agglutinates in H4-Aβ42 conditioned medium confirmed that bacterial cells were also bound and linked by fibrils (fig. S3F).

Epifluorescence micrographs of Thioflavin S–stained late-stage (>12 hours after infection) H4-Aβ42 yeast aggregates displayed the enhanced fluorescence and red shifts that mark the presence of amyloid fibrils (Fig. 5A). Enhanced fluorescence was not observed for negative control yeast agglutinates (Fig. 5A). Thioflavin S fluorescence within H4-Aβ42 yeast aggregates colocalized with the signal for anti-Aβ immunoreactivity (Fig. 5B). Congo red–stained H4-Aβ42 yeast aggregates also showed birefringence under polarized light, another marker for β-amyloid (fig. S7). Scanning electron microscopy (SEM) micrographs of yeast aggregates from H4-Aβ42 medium revealed an irregular material adhering to cell surfaces not present in *Candida* pellets prepared by centrifugation in Aβ-free medium (Fig. 5C). Analysis of the *Candida* cell surface by TEM revealed the adhering material to be filamentous and immunoreactive to anti–Aβ-Au (Fig. 5D). Co-incubation of soluble synthetic Aβ40 peptide abolished anti–Aβ-Au binding. Collectively, the data are consistent with microbial agglutination and entrapment mediated by Aβ fibrillization in our cell culture infection model.

β-Amyloid mediates pathogen entrapment in GMC101 nematodes and 5XFAD mice

We also investigated infection-associated Aβ fibrillization in our nematode and mouse infection models. Consistent with Aβ targeting and binding to yeast cells in our cell culture model, *Candida* in the gut of recently infected (2 hours after ingestion) GMC101 nematodes were labeled by anti–Aβ-Au nanoparticles (Fig. 6A). Yeast cells in the gut of the control CL2122 nematode were not labeled by anti–Aβ-Au (fig. S8A). Aβ fibrillization in GMC101 worms is normally confined to the body wall muscle. However, compared to infection-free nematodes,

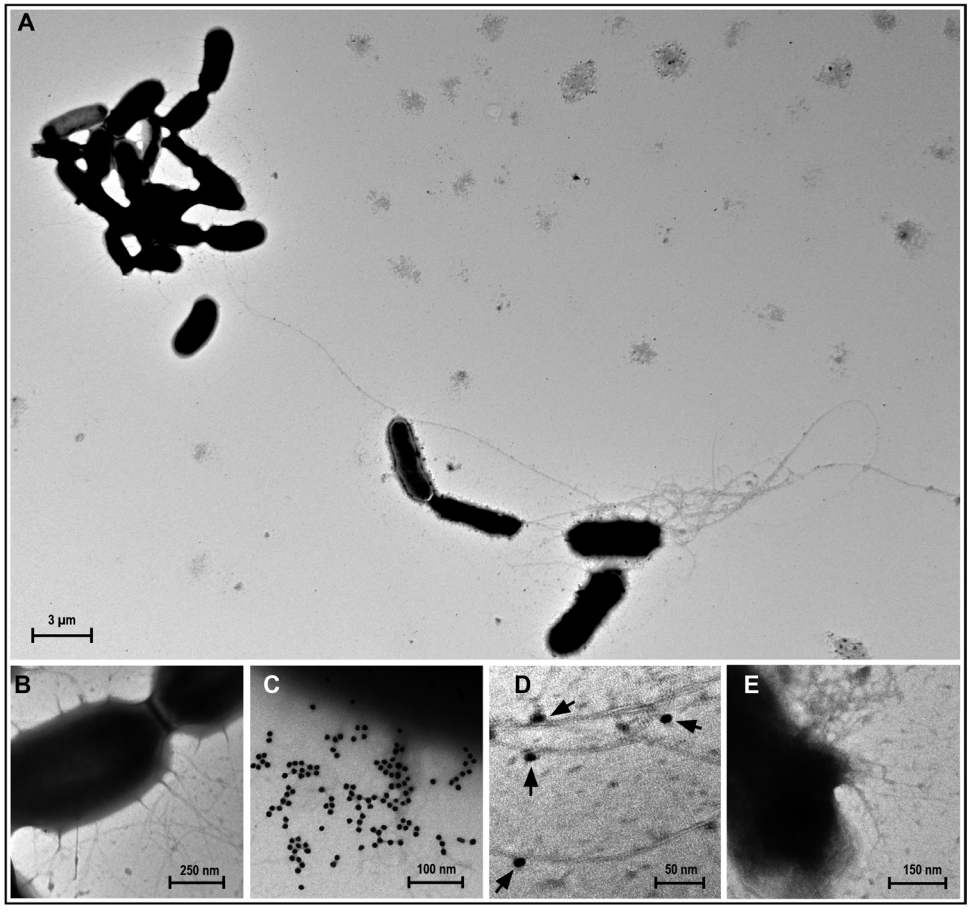

Fig. 4. β-Amyloid fibrils propagate from yeast surfaces and capture *Candida* in H4-Aβ42 medium. Early-stage *C. albicans* aggregates harvested from H4-Aβ42 conditioned medium were probed with α–Aβ-Au nanoparticles and analyzed by TEM. (**A**) Yeast agglutination is mediated by fibrillar structures. The micrograph shows fibrils binding cells within yeast aggregates and linking *C. albicans* clusters. (**B**) Fibrillar structures extending from yeast cell surfaces. (**C** and **D**) α–Aβ-Au nanoparticle labeling of short fibrillar structures extending from *C. albicans* surfaces and long fibrils running between yeast clumps. (**E**) Absorption experiment showing ablated α–Aβ-Au binding of fibrils extending from yeast in the presence of soluble synthetic Aβ peptide. Data are consistent with specific α–Aβ-Au labeling of β-amyloid fibrils. Micrographs are representative of data from three replicate experiments and multiple discrete image fields (table S1A).

GMC101 worms with late-stage *Candida* infection showed enhanced Thioflavin S fluorescence in nonmuscle tissue, including the gastrointestinal tract (Fig. 6B). High-resolution micrographs of yeast cells in the gastrointestinal tract of GMC101 nematodes revealed clumped *Candida* embedded in the material that showed enhanced fluorescence after Thioflavin S staining (Fig. 6C) and was labeled by anti-Aβ antibodies (Fig. 6D). Consistent with Aβ-specific labeling, anti-Aβ signal (fig. S2B) and enhanced Thioflavin S fluorescence (fig. S8B) were absent from uninfected or *Candida*-infected negative control CL2122 nematodes that did not express Aβ. Findings for *C. albicans*–infected GMC101 nematodes were consistent with the agglutinating and entrapment roles of Aβ fibrils observed in our cell culture infection models. Thus, Aβ fibrillization on the surface of yeast cells infecting the gut of GMC101 nematodes may mediate the resistance to infection observed for these worms.

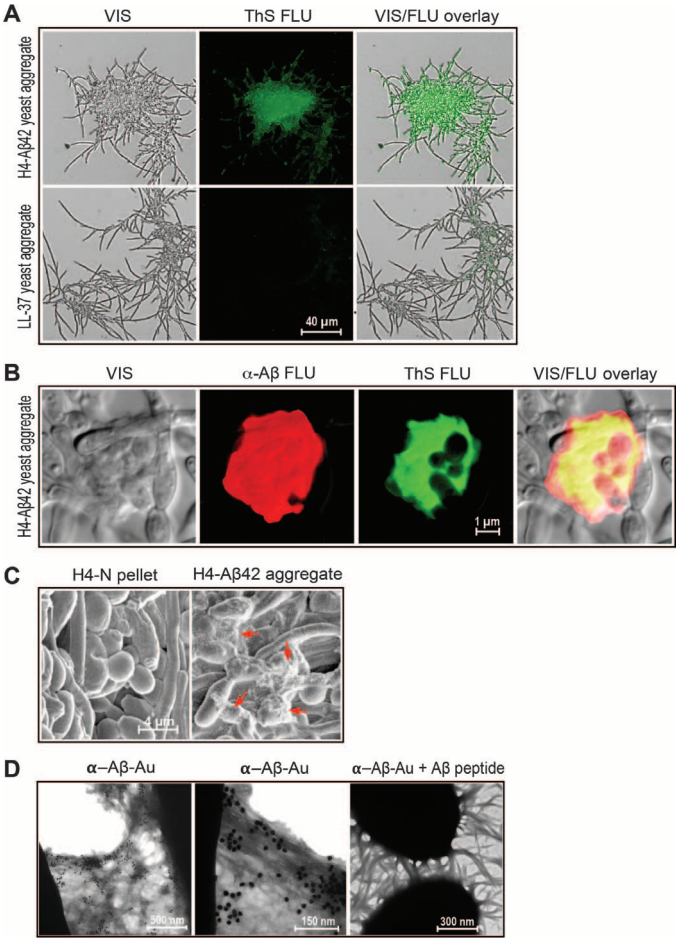

Fig. 5. *Candida* cells are entrapped by Aβ in H4-Aβ42 culture medium. After overnight incubation with H4-Aβ42 medium, yeast (*C. albicans*) aggregates were harvested and probed for β-amyloid markers. (**A** and **B**) Visible yeast aggregates (VIS), yeast aggregates stained with green fluorescent Thioflavin S (ThS FLU), yeast aggregates probed with red fluorescent anti-Aβ (α-Aβ FLU) antibodies, and superimposed images (VIS/FLU overlay). Yeast aggregates generated with the control synthetic LL-37 peptide (A) are negative for Thioflavin S–enhanced fluorescence. (B) Yellow denotes colocalization of anti-Aβ and Thioflavin S signals. Colocalization of these signals is the hallmark of Aβ. (**C**) SEM analysis revealed fibrous material in H4-Aβ42 yeast aggregates that is absent from control *C. albicans* pellets prepared by centrifugation in H4-N medium. (**D**) H4-Aβ42 yeast aggregates incubated with immunogold nanoparticles coated with anti-Aβ antibodies (α–Aβ-Au) and analyzed by TEM. The first and second panels show labeling of fibrous material by α–Aβ-Au. The third panel shows inhibition of α–Aβ-Au nanoparticle binding by soluble synthetic Aβ peptide (α–Aβ-Au + Aβ peptide), consistent with specific labeling of β-amyloid. Micrographs are representative of data from two or more replicate experiments and multiple discrete image fields (table S1A).

Four-week-old 5XFAD mouse brain is normally negative for β-amyloid deposits (*12*). However, Thioflavin S and anti-Aβ staining of 5XFAD mouse brain revealed widespread β-amyloid deposition 48 hours after infection with *S.* Typhimurium (Fig. 7, A and B). Moreover, anti-*Salmonella* and β-amyloid signal colocalized in the 5XFAD mouse brain, suggesting that bacterial cells may have induced Aβ fibrillization. TEM analysis also revealed that bacterial cells were embedded in fibrous material labeled by anti–Aβ-Au nanoparticles in 5XFAD but not wild-type mouse brain sections (fig. S8). A video of Z-section projections rotating through 360° shows that bacteria are not confined to the surface of Aβ accretions but are embedded within the β-amyloid deposits (video S1). Consistent with fibrillization driven by proliferation of *S.* Typhimurium cells, β-amyloid deposits were absent from sham-infected 1-month-old 5XFAD control mice injected with heat-killed bacteria. Thioflavin S staining and anti–β-amyloid antibodies did not label mouse brain from negative control nontransgenic littermates (Fig. 7A).

DISCUSSION

Our findings are consistent with a potential protective role for Aβ in vivo as an AMP. Expression of Aβ was associated with increased host survival in cell culture, nematode, and mouse infection models (Figs. 1 and 2). Low Aβ expression was associated with higher mortality after infection of APP-KO mice. Our data are consistent with a protective role for Aβ in innate immunity that uses a classic AMP mechanism characterized by reduced microbial adhesion to host cells and agglutination and entrapment of microbes by Aβ fibrils. Moreover, well-characterized Aβ activities mediate the peptide's antimicrobial actions. However, these same properties, oligomerization, fibrillization, and carbohydrate binding, are also linked to Aβ's pathophysiology. Whereas a protective/damaging duality is a new proposition for Aβ's activities, this is not the case for classical AMPs. For example, LL-37 offers a germane model for the potential pathological consequences of normally protective AMP actions. LL-37 is essential for normal immune function, and low expression leads to lethal infections (*37*). However, at elevated concentrations, LL-37 is cytotoxic to host cells, particularly smooth muscle cells (*38*). The cytotoxic and proinflammatory activities of LL-37 are implicated in the pathogenesis of several major late-life diseases, including rheumatoid arthritis, lupus erythematosus, and atherosclerosis (*39*). Thus, a normally protective Aβ activity spectrum that, when dysregulated, also leads to AD pathology is consistent with the actions of classical human AMPs.

Adhesion blocking and agglutination activities are distinct from AMP microbicidal activities, which typically require micromolar concentrations of peptide and involve different mechanisms (*22*). The adhesion inhibition and agglutination activities that we observed in vitro for cell-derived Aβ (Fig. 3) fall within physiological concentration ranges reported for normal human CSF (1 to 5 ng/ml). Consistent

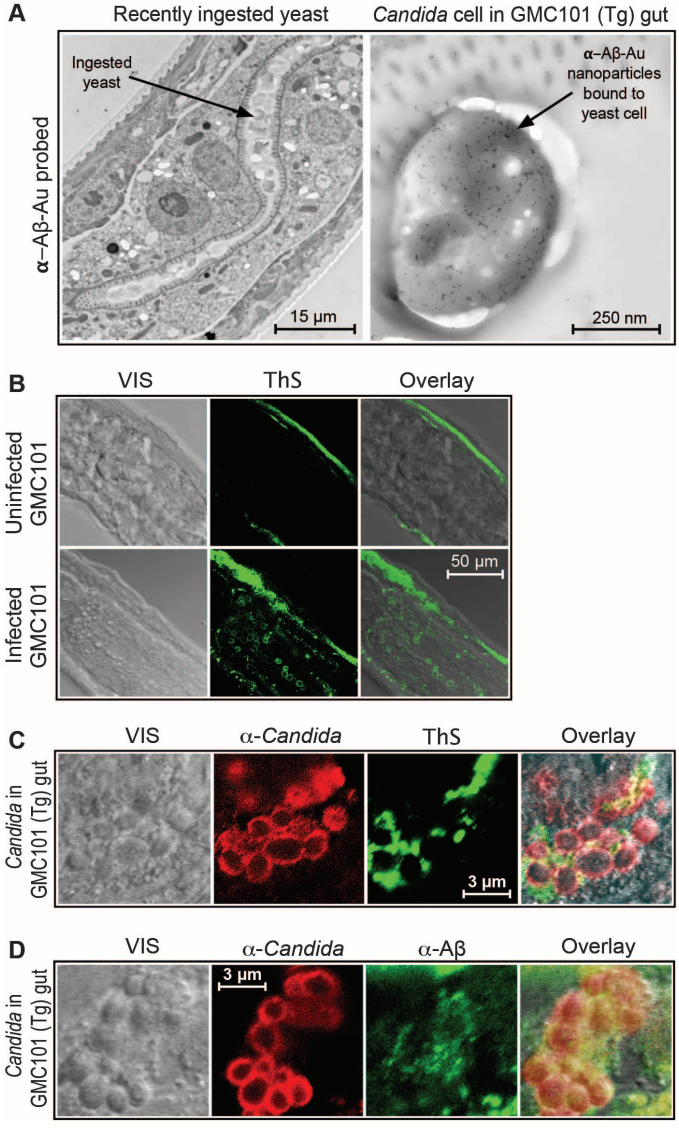

Fig. 6. Intestinal infection with *Candida* induces Aβ fibrillization in transgenic GMC101 nematode gut. Aβ42-expressing GMC101 *C. elegans* were infected with *C. albicans* (*Candida*) and probed for anti-Aβ immunoreactivity and β-amyloid markers using TEM and confocal fluorescence microscopy (CFM). (**A**) Micrograph shows positive labeling of yeast cell surface in GMC101 worm gut by immunogold nanoparticles coated with anti-Aβ antibodies (α–Aβ-Au) after *Candida* ingestion. (**B** to **D**) Visible (VIS) and fluorescence signals from freeze-fracture nematode sections with advanced *Candida* infections. (B) Comparison of uninfected and infected worms. (C and D) Thioflavin S and anti-Aβ staining for gut yeast aggregates. Signals include anti-*Candida* immunoreactivity (α-*Candida*), Thioflavin S–enhanced fluorescence (ThS), anti-Aβ immunoreactivity (α-Aβ), and superimposed (Overlay) signals. Yellow denotes signal colocalization. Uninfected and infected CL2122 nematode controls were negative for anti-Aβ immunoreactivity and enhanced Thioflavin S fluorescence (figs. S2 and S8). Micrographs are representative of data from three or more replicate experiments and multiple discrete image fields (table S1B).

with a normal in vivo protective role, the highest cerebral concentrations of Aβ are in the leptomeninges (10 to 50 ng/ml) (*40*), the brain's first line of defense against infection and a tissue enriched for LL-37 and other innate immune proteins (*41*). The high specific activity observed for cell-derived material is consistent with our previous finding that Aβ in human brain extracts is a potent anti-*Candida* agent (*3*). Classical AMP expression can be either constitutive or inducible (*5*). In our transgenic mouse, nematode, and cell culture models, constitutive expression of Aβ is maintained artificially. Hence, our models are not suitable for testing whether infection normally results in Aβ up-regulation. However, data from other investigators suggest that Aβ may be an inducible AMP. Host cell exposure to herpes simplex virus–1 (*42*), HIV-1 (*42*), spirochetes (*43*), or Chlamydia (*44*, *45*) increases Aβ expression.

In in vitro assays, cell-derived and synthetic Aβ oligomers were more potent against *Candida* than were monomeric forms (Fig. 3, C to F, and fig. S5C). The specific activities of synthetic ADDLs, although higher than nonoligomerized peptide, remain lower than cell-derived Aβ species. Peptide posttranslational modifications may enhance the AMP activity of cell-derived Aβ oligomers. However, oligomer conformation is also likely to play a key role. Neurotoxicity has been shown to be highly dependent on the arrangement of Aβ peptides within oligomeric assemblies. Oligomer morphology may also modulate Aβ's protective antimicrobial activities. Protocols for preparing ADDLs and other synthetic Aβ assemblies are optimized for oligomer populations with neurotoxic, not antimicrobial, activities. Future protocols optimized for enhanced AMP activities may generate soluble synthetic Aβ oligomers with potencies that approach that of cell-derived material.

Aβ pathophysiology is thought to arise from an abnormal propensity to generate soluble oligomers. However, oligomerization is not a pathogenic behavior for AMPs, and it plays a key role in normal protective activities across this diverse group of proteins, including microbe agglutination and entrapment (*35*), the targeting (*26*, *30*) and disruption of microbial cell membranes (*4*, *46*), resistance to bacterial proteases (*26*, *27*, *46*), and expanding of the molecular diversity and protective functions of AMP families without commensurate genome expansion (*28*, *29*). Our data and the widespread involvement of oligomerization in the protective actions of AMPs suggest that the brain's pool of soluble Aβ may normally include physiologically functional oligomeric species that mediate protective antimicrobial activities. The intrinsic polymorphic stoichiometry of Aβ oligomers may also play a protective physiological role. As has been shown with classical AMPs, diverse polymorphic oligomer pools target a broader spectrum of pathogens and are more resistant to AMP-targeting microbial proteases than are homogeneous peptide populations.

The lectin activity of Aβ oligomers is thought to promote brain amyloidosis (*34*). Studies to date have focused on accelerated Aβ fibrillization induced by binding of endogenous brain proteoglycans and glycosaminoglycans. However, our findings suggest that Aβ oligomers also bind to microbial carbohydrates with high affinity (Fig. 3, G to J). Carbohydrate-binding activity among AMPs is widespread and normally protective, playing a key role in helping peptides to recognize and bind to microbial pathogens (*22*). Heparin-binding AMPs have high affinities for the unique microbial carbohydrates found in cell walls but also bind to host glycosaminoglycans (*47*). Consistent with our findings for Aβ, binding of classical AMPs to microbial carbohydrates can lead to rapid peptide fibrillization and amyloid-mediated antimicrobial activities (*48*). Dysregulated carbohydrate binding by

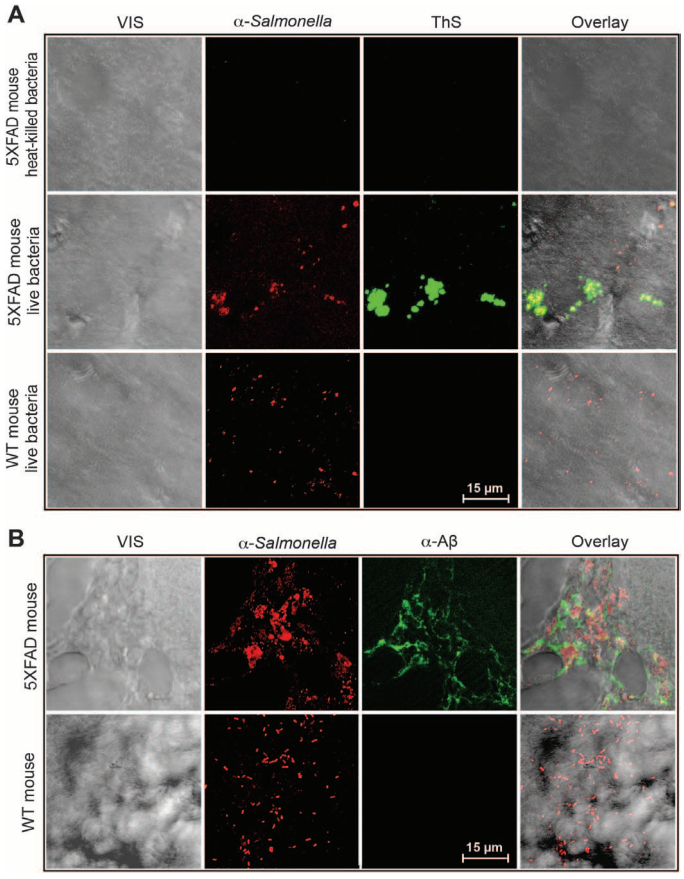

Fig. 7. Infection-induced β-amyloid deposits colocalize with invading *S.* Typhimurium cells in 5XFAD mouse brain. Four-week-old WT mice or transgenic 5XFAD animals expressing high levels of human Aβ were injected intracerebrally with viable *S.* Typhimurium bacteria. Mice were also injected with heat-treated *S.* Typhimurium cell debris as a negative control for the injection procedure. (**A** and **B**) Mouse brain sections were prepared 24 (A) or 48 hours (B) after infection. Signals shown include visible (VIS), anti-*Salmonella* immunoreactivity (α-*Salmonella*), enhanced Thioflavin S fluorescence (ThS) or anti-Aβ immunoreactivity (α-Aβ), and superimposed (Overlay) signals. Panels are representative images of multiple images captured as Z-sections using CFM. Yellow denotes signal colocalization (Z-series projections showing β-amyloid surrounding and entrapping bacterial colonies in a rotating three-dimensional section of 5XFAD mouse brain are also included in video S1). Micrographs are representative of data from three replicate experiments and multiple discrete image fields (table S1C).

Aβ may play a role in AD amyloidogenesis. However, a normal role as an AMP would suggest that polymeric microbial cell surface carbohydrates may be the normal in vivo target for the heparin-binding activity of oligomeric Aβ species.

Long recognized as a key defensive strategy among lower organisms, AMP-mediated microbial agglutination is also emerging as an important part of human immunity (*49*). AMP fibrillization appears to play a central role in this important protective activity (*35*). Most recently, in vivo fibrillization of HD6 has been shown to mediate not only agglutination but also microbial entrapment within an amyloid fibril network (*36*). Our findings suggest that fibrillization is also involved in Aβ-mediated agglutination and leads to the entrapment of microbial cells by Aβ fibrils. On the basis of our findings, we propose a three-stage model for the protective activity of Aβ in vivo. Our model parallels the agglutination and entrapment actions of amyloidogenic HD6 (*36*). First, the VHHQKL heparin-binding domain of Aβ mediates targeting and binding of soluble oligomeric species to cell wall carbohydrates (fig. S10A). Bound oligomers then provide a nidus and anchor for Aβ fibril propagation. Second, growing protofibrils interfere with microbial adhesion to host cells (fig. S10B). Third, Aβ fibrils link, agglutinate, and then entrap the unattached microbial cells in a protease-resistant network of β-amyloid (fig. S10C). Consistent with our model for the antimicrobial activities of Aβ, classical human AMPs have also been shown to generate amyloid fibrils on microbial surfaces that agglutinate pathogens and inhibit infection (*35*).

Consistent with our AMP model for Aβ, APP-KO mice show a trend for reduced pathogen resistance (Fig. 1E). However, the increase in infection-driven mortality among APP-KO mice was less marked than the increase in survival observed in the 5XFAD mouse model (Fig. 1A). For AMP-deficient models, immune impairment is often moderate because redundant activities among related members of AMP families can partially offset the loss of protection associated with low expression of individual AMP species (*50*). The well-studied human AMP LL-37 that serves as our model for Aβ's AMP activity (*3*) is a member of the cathelicidin protein family. In humans, serious immunodeficiency associated with low LL-37 expression typically leads to fatal infections in childhood if untreated (*37*). However, mice lacking the murine LL-37 precursor protein (mCRAMP) show only a modest increase in mortality (≈10%) due to bacterial meningitis (*51*). Conversely, survival with infection among transgenic mice overexpressing human LL-37 is increased several-fold (*52*). APP-KO mice generate at least two Aβ homologs from amyloid precursor-like protein 1 (APLP1) and 2 (APLP2), which may help to mitigate loss of Aβ-mediated protection (*53*). Consistent with this model, APP, APLP1, and APLP2 and their nonamyloidogenic processing products show extensive functional redundancy (*54*), likely because of the gene duplication origin for this protein family. APP-KO mice also have an important additional limitation as models for the loss of Aβ-mediated protection. APP itself may be involved in central nervous system (CNS) immunity (*55*). It remains unclear how loss of activities normally mediated by full-length APP can be excluded as the source of attenuated infection resistance in APP-KO mice.

Genetically modified mice that lack proteases [BACE1 (β-site APP cleaving enzyme 1) and BACE2] for generating the Aβ family of peptides provide an alternative Aβ-null model. Consistent with our data, knockout BACE-KO mice that lack BACE have been reported to have marked immunodeficiency. Whereas neonatal mortality is below 2% under sterile conditions, in less stringently antiseptic environments, up to half of pups born to BACE-KO mice die from infections within the first 2 weeks of life (*56*). Benchmark tests for adaptive immunity have failed to identify defects in the response of BACE-KO mice to immune challenges. Findings for BACE-KO mice appear consistent with an innate immune deficiency and a possible normal protective role for Aβ. However, as with APP-KO mice, it is unclear how to demonstrate that the immunodeficiency in BACE-KO mice is specific for a loss of members of the Aβ family of peptides. Additional data are required to conclusively link the etiology of BACE-KO mouse immunodeficiency to low Aβ.

Our findings for Aβ and β-amyloid may have corollaries for amyloidopathies beyond AD. Protein fibrillization may be important not only for Aβ's AMP activities but also for the normal actions of other amyloidosis-causing proteins. An association between amyloidosis and chronic bacterial infections has been recognized for almost a century (*57*), but the potential protective activities of host-generated amyloid have only recently emerged (*4*, *35*, *58*). At least six amyloidosis-associated peptides show antimicrobial activities, including amylin (*59*), atrial natriuretic factor (*9*), prion protein (*60*), cystatin C (*61*), lysozyme (*5*), and superoxide dismutase (*62*). Conversely, host AMPs have been identified that generate protective amyloids localized to infection sites (*4*). AA-type amyloidosis involves both systemic deposition of the acute-phase opsonin AMP serum amyloid A and has an infection-driven etiology (*63*). It remains to be determined whether serum amyloid A or other amyloidosis-causing AMPs also engage in nonpathogenic fibrillization pathways that help to protect against infection. However, should this prove to be the case, Aβ may be the first member of a new class of AMPs in which amyloid-generating activities protect against local infections but can also lead to widespread pathological amyloidosis.

If confirmed, our model carries important implications for understanding the pathogenesis of amyloidosis in AD. Excessive β-amyloid deposition may arise not from an intrinsically abnormal propensity of Aβ to aggregate but instead may be mediated by dysregulation of the brain's innate immune system, for example, the consequence of an immune response mounted to microbial or sterile inflammatory stimuli. Our new model is congruent with the amyloid hypothesis and the importance of Aβ and β-amyloid in the neurodegenerative cascade of AD. However, our model would shift the modality of Aβ's pathophysiology from abnormal stochastic behavior toward dysregulated antimicrobial activities.

Our study used genetically modified cell and animal models to generate data consistent with a normal physiological role for Aβ as an AMP. However, it remains unclear from these data how important a role Aβ plays in normal infection resistance. To address this question, additional data will be needed from wild-type animals modeling common physiological routes of infection. Further investigation will also be needed to clarify the extent to which the normal antimicrobial activities of Aβ identified in our study affect AD pathology.

It is important to emphasize that although infection of 5XFAD mice with *S.* Typhimurium seeded and accelerated β-amyloid deposition, the presence of a CNS infection is not implicit in our proposed AD amyloidosis model. Our work has identified what we believe is the normal role of Aβ. What drives widespread β-amyloid deposition in AD remains unclear. Among sterile inflammatory diseases, dysregulated innate immune responses rather than infections are emerging as drivers of pathology. Notably, two of the three confirmed AMP amyloidopathies are not linked to obvious infections (*4*, *9*, *64*). However, a large body of data accrued over nearly a century suggests that genuine infection may also play a role in AD etiology (*65*). Moreover, although a causal link to amyloidosis remains to be conclusively demonstrated, recent epidemiological findings have given increased prominence to the "infection hypothesis," including studies linking brain fungal infection to AD (*17*, *18*) and data showing that risk for the disease increases with infectious burden (*66*). Our findings do not constitute direct evidence of a role for infection in AD etiology. However, they do suggest a possible mechanism for pathogen-driven β-amyloid amyloidosis. Our data also suggest the possibility that a range of microbial organisms may be able to induce β-amyloid deposition, a possible reason for why a single pathogen species has not yet been identified that is overwhelmingly associated with AD. Future studies systematically characterizing microbial pathogens (viral, bacterial, and fungal) in the brains of AD patients, for example, by RNASeq, will be necessary to further interrogate whether specific clinical pathogens seed β-amyloid as part of the brain's innate immune system. In any case, whether infectious or sterile inflammatory stimuli drive AD pathology, the pathways that regulate innate immunity in the brain may offer significant new targets for therapeutic intervention.

MATERIALS AND METHODS

Study design

Protective activities associated with Aβ expression were investigated in murine, nematode, and cell culture models of infection. Transgenic mice, nematode, and cell culture models were used that constitutively express human Aβ at high levels. Experiments also included a null-Aβ mouse model. Modulation of infection resistance with peptide expression is considered a hallmark for identity as an AMP. Initial experiments tested for Aβ-mediated increase (high-expression models) or decrease (null-Aβ mice) in survival after infection. End points were death for cultured cells and nematodes and moribundity for mice in accordance with Institutional Animal Care and Use Committee guidelines. Experiments were conducted blind as to cell, nematode, and mouse genotypes. The mechanism of protection afforded by high Aβ expression was then characterized in our cell culture monolayer infection model. We have previously shown parallels between Aβ activities and LL-37, a highly characterized human AMP. LL-37 was used as a model to elucidate the mechanisms for Aβ targeting, adhesion inhibition, and agglutination activities against microbial cells. Finally, nematode and mice models were tested to confirm in animals the potential protective microbial entrapment role of Aβ fibrillization revealed by cell culture experiments. Figure legends include details of replicate experiments used to generate data sets.

Monomeric and oligomeric synthetic peptide preparation

Synthetic Aβ1–40 (Aβ40), Aβ1–42 (Aβ42), scrambled Aβ42 (scAβ42), and LL-37 peptides were prepared and purified by J. I. Elliott at Yale University (New Haven, CT) using solid-phase peptide synthesis. Bulk powdered Aβ peptides were initially dissolved and incubated (18 hours) at room temperature (RT) in 30% trifluoroethanol (1 mg/ml) before lyophilization and storage (−20°C) under nitrogen. Before experimentation, dried peptide films were solubilized in 10 mM NaOH. For preparation of monomeric Aβ stocks, peptide solutions were diluted into phosphate-buffered saline (PBS) and fractionated by size exclusion chromatography, and peak monomer fractions (3 to 6 kD) were pooled. Monomer stocks were stored on ice at 100 μM and used within 2 hours of preparation. Synthetic Aβ42 oligomer preparations (ADDLs and protofibrils) were generated from NaOH peptide stocks using established protocols (*67*). Peptide concentrations in stock solutions were determined by bicinchoninic acid protein assay and confirmed in experimental serial dilutions by densitometry analysis of anti-Aβ immunoblots.

Candida inoculants and lawns

Freezer stocks of *C. albicans* strain 90028 were obtained from the ATCC. *C. albicans* stocks were maintained on yeast extract peptone

dextrose (YPD) agar at 4°C with subculture to fresh plates every 2 weeks.

C. elegans pathogenicity plates were prepared by streaking (10 μl) sterile 35-mm tissue culture plates (BD Falcon) with yeast grown overnight (30°C) in YPD broth. Plates were incubated at 25°C for 2 hours to generate *C. albicans* lawn.

Synchronized hyphal yeast for cell culture experiments were prepared by single-colony transfer of *C. albicans* stock to 5 ml of minimal sugar medium (Formedium) and 48-hour static incubation at RT (*68*). After pelleting (1750 relative centrifugal force for 2 min) and PBS washing, starved yeast were resuspended in RPMI 1640 medium (HyClone) and concentration was adjusted to 2.5×10^6 cells/ml. Stock yeast in RPMI were diluted 10-fold into unconditioned culture medium immediately before inoculation of host cell slide or culture plate wells. Yeast concentration in inoculates was determined using a Bio-Rad TC20 automated cell counter and confirmed by counting CFU after serial dilution and streaking on agar.

S. Typhimurium inoculants

S. enterica serotype Typhimurium SL1344 stocks were provided by B. Cherayil (Mucosal Immunology Department, Massachusetts General Hospital, Boston, MA). Colonies were maintained on agar and subcultured to fresh plates every 3 weeks. Inoculant stocks were prepared by single *S.* Typhimurium colony to transfer to Luria-Bertani agar with streptomycin (100 μg/ml) and incubation overnight in a shaker incubator (225 rpm at 37°C). After PBS washing, pelleted (10,000*g* × 2 min) bacteria were resuspended in inoculation medium and diluted to required concentration. Bacterial concentrations in stocks were determined by comparing inoculum turbidity to McFarland turbidity standards and confirmed by streaking on agar and counting CFU.

For mouse experiments, *S.* Typhimurium inoculants were pathologized before infection by incubation in Luria broth with streptomycin (100 μg/ml) overnight at 37°C. Pathogenicity plates for *C. elegans* were prepared by streaking inoculate (10 μl) onto *Pseudomonas aeruginosa*– and *S. enterica*–killing assay plates and overnight incubation at 37°C. For host cell monolayers, inoculant was added directly to culture medium.

Immunodepletion

Protein G Plus Agarose slurry (Pierce) was pelleted, washed, and incubated for 2 hours at RT with 4G8 (epitope: Aβ17–24) monoclonal antibody (mAb) (Covance) or control mouse IgG in PBS. After washing, beads were incubated with medium samples for 2 hours at RT under conditions equivalent to 10 μg of antibody per milliliter of medium. Beads were pelleted, and soluble fractions were removed, filtered (0.2 μm), and assayed to confirm Aβ depletion.

Aβ binding ELISA

The wells of 96-well plates were coated with live yeast by overnight incubation (37°C) with synchronized *C. albicans* (50 to 250 CFU per well) in RPMI medium (200 μl per well). Wells were washed to remove unattached yeast, and adhering *C. albicans* cells were then killed and covalently fixed in place by incubation (15 min at RT) with 4% paraformaldehyde. Wells were blocked (2 hours at RT) with 2% bovine serum albumin (BSA) in PBS before incubation with experimental samples. Bound Aβ in wells was detected immunochemically by incubation (overnight at 4°C) with α–Aβ42-HRP (horseradish peroxidase) (Covance) diluted 1:1000 in blocking buffer and development with 100 μl of chemiluminescence reagent (Pierce). Wells were washed (five times) with PBS between incubations.

Mouse infection model

Female 5XFAD (*12*) APP/PS1 doubly transgenic mice co-overexpress and co-inherit FAD mutant forms of human APP (the Swedish mutation: K670N/M671L; the Florida mutation: I716V; the London mutation: V717I) and PS1 (M146L/L286V) transgenes under transcriptional control of the neuron-specific mouse Thy-1 promoter (Tg6799 line). 5XFAD lines (B6/SJL genetic background) were purchased from The Jackson Laboratory and maintained by crossing heterozygous transgenic mice with B6/SJL F1 breeders. All 5XFAD transgenic mice were heterozygotes with respect to the transgene. Animal experiments were conducted in accordance with institutional and National Institutes of Health guidelines.

One-month-old mice received a single injection of 65,000 CFU (0.18 to 0.20 μl) of *S.* Typhimurium suspension at anterior/posterior, −1.6; medial/lateral, +1.5; dorsal/ventral, −1.6/−1.1/−0.7 using a 5-μl Hamilton syringe with a 30-gauge needle attached to a digital stereotaxic apparatus and an infusion pump at a rate of 0.15 μl/min. After infusion was completed, the needle remained in place for 10 min before slow withdrawal. Mice were given food and water on the cage floor starting 24 hours after the injection. Control sham infections used *S.* Typhimurium heat-killed before injection.

Clinical scores were recorded every 8 hours according to modified grading criteria for mouse encephalomyelitis (*69*, *70*). Clinical criteria are summarized in fig. S1A. Clinical progression was followed to moribundity, and then mice were sacrificed. Scores were recorded for each mouse and expressed as means ± SEM.

Mouse tissue preparation and sectioning

For immunofluorescence, mice were deeply anesthetized with a mixture of ketamine and xylazine and perfused transcardially with 4% paraformaldehyde in cold PBS. Brains were postfixed overnight and then transferred into a 30% sucrose solution until sedimented. Coronal sections (40 μm) were cut from an ice-cooled block using a sliding microtome (Leica). Sections were stored at −20°C in cryoprotective buffer containing 28% ethylene glycol, 23% glycol, and 0.05 M phosphate until processing for analysis.

Immunofluorescence labeling of mouse sections

Immunofluorescence labeling was performed as previously described (*12*). Primary antibodies include rabbit anti-GFAP (1:500, Dako) for astrocytes, rabbit anti-ionized calcium-binding adaptor molecule 1 (Iba1, 1:500, Wako) for microglia, and anti-*Salmonella* polyclonal rabbit for *S.* Typhimurium. Bound primary antibodies were detected with anti-rabbit Alexa Fluor 594 (Invitrogen, 8889S). Cell nuclei in sections were stained with TO-PRO-3 iodide (1:500, Life Technologies).

Immuno- and Thioflavin S–costained mouse sections

Immunofluorescence labeling was performed as described previously (*71*). Briefly, sections were incubated with primary anti-*Salmonella* polyclonal rabbit IgG (1:1000) (PA1-7244, Thermo Fisher Scientific), followed by secondary anti-rabbit Alexa Fluor 594 (1:500) (Invitrogen, 8889S) antibodies. For Aβ staining, sections were incubated with mouse mAbs 3D6 (Eli Lilly) (mouse brain sections) or 4G8 (nematode sections). Bound anti-Aβ antibodies were detected by incubation with anti-mouse Alexa Fluor 488 (1:500) (Life Technologies, A11001)

antibodies (Invitrogen). After immunostaining, free-floating sections were incubated (8 min) with 0.002% Thioflavin S in tris-buffered saline (TBS), rinsed twice for 1 min in 50% methanol washed for 5 min in TBS, and mounted with ProLong Gold antifade reagent (Life Technologies). Stained sections were analyzed by CFM (Leica TCS SL, Leica Microsystems).

C. elegans model

Two previously described transgenic *C. elegans* strains were used in experiments. GMC101, *dvIs100* [pCL354(*unc-54:DA-Aß1-42*) + pCL26 (*mtl-2: GFP*)] nematodes express human Aβ42 in body wall muscle and GFP in intestinal cells (*14*). Control *C. elegans* CL2122 *dvIs15*(*mtl-2: GFP*) nematodes express GFP but not the Aβ42 peptide (*14*). Worms were synchronized before experimental treatments according to established protocols (*72*). Briefly, unhatched eggs were released by treating gravid worms with bleach. After an overnight incubation, arrested L1 larvae were added to *Escherichia coli* OP50 lawns and incubated at 20°C to generate synchronized L4 larval (48 hours) or adult (60 hours) nematodes.

For infection experiments, 100 to 150 synchronized L4 stage worms were incubated (2 hours at 25°C) on *C. albicans* lawns, washed with M9 buffer to remove surface *C. albicans*, and transferred to six-well culture plates containing 1.5 ml per well of incubation medium [79% M9 buffer, 20% brain-heart infusion, cholesterol (10 μg/ml) in ethanol, and kanamycin (90 μg/ml)]. Nematodes were incubated at 25°C and monitored daily for the distinctive distention and penetrative filamentation that characterize *Candida*-induced mortality.

Nematode freeze-fracture and immunostaining

Worms (L4) were transferred dropwise to poly-lysine–coated slides and covered with a coverslip. Gentle pressure was applied to the coverslip before the slide assembly was placed on a metal block and flash-frozen using liquid nitrogen. The coverslip was flicked off, and fractured samples were fixed by 5-min incubations with absolute alcohol, followed by acetone. Dried samples were ringed with petroleum jelly and covered with a second coverslip. Slide staining was performed in a wet chamber. For immunostaining, slides were blocked for 15 min with blocking buffer [10% Tween and powdered milk (0.2 g/ml) in PBS] and then incubated (1 hour at RT) with rabbit polyclonal anti-*Candida* antibody (Abcam, ab20028) and/or anti-Aβ mAb 4G8. After washing, slides were incubated with anti-rabbit and/or anti-mouse antibodies conjugated to Alexa Fluor 568 and Alexa Fluor 488 fluorescent dyes (Life Technologies), respectively. For Thioflavin S staining, slides were incubated for 1 hour at RT with dye solution and PBS-washed. Specimens were incubated with ProLong Gold antifade reagent (Life Technologies) before viewing by CFM.

Host cell monolayer model

Host cell monolayers were prepared from nontransformed and transformed human neuroglioma (H4) or CHO cell lines. Stable transformed H4 cell lines that secrete Aβ40 (H4-Aβ40) or Aβ42 (H4-Aβ42) without overexpression of the APP have been described previously (*19*). Stable transformed CHO-CAB cells coexpressing human ATCC Swedish mutation and BACE1 were generated by transfecting a pcDNA3.1-BACE1-myc construct into CHO-APP751 cells that overexpress mutant APP751 (K670N/M671L: Swedish mutation) (*20*).

Nontransformed H4-N and CHO-N cell lines were maintained in complete medium containing Dulbecco's modified Eagle's medium (DMEM), 10% fetal bovine serum (FBS), 2 mM L-glutamine, 100 U penicillin, and streptomycin (100 μg/ml). Complete medium for transformed H4-Aβ40 and H4-Aβ42 cells included hygromycin (150 μg/ml) and media for CHO-CAB Zeocin (200 μg/ml) and G418 (200 μg/ml).

To prepare experimental HCMs, trypsinized host cells suspended in antibiotic-free DMEM with 5% FBS and 2 mM L-glutamine were transferred (300,000 and 500,000 cells/ml for H4 and CHO lines, respectively) to the wells of Lab-Tek eight-chamber glass slides (Thermo Scientific) (200 μl per well) or 96-well culture plates (100 μl per well) and incubated for 24 hours. Cell confluence in chamber slides and plate wells was confirmed by microscopic examination. Automated cell counter analysis of well trypsin extracts confirmed that, in control uninfected cell monolayers, nontransformed and transformed cell numbers did not diverge by more than 6% before infection or after the final experimental incubation (fig. S4D).

Nontransformed and transformed culture media were conditioned for 36 hours before inoculation with *Candida*. HCMs in culture plates were infected by addition of *Candida* inoculant aliquots (10 μl) containing 2000 or 250,000 CFU, respectively. For host cell survival experiments, *Candida* were incubated with H4 and CHO cells for 28 and 36 hours, respectively. HCMs were then washed and assayed for host cell survival.

Host cell BrdU labeling

Subconfluent nontransformed and transformed H4 and CHO cells were incubated overnight (10-cm culture dishes) in complete culture medium containing 10 mM BrdU. Confluent BrdU-labeled cell cultures were PBS-washed (three times) to remove free BrdU, then trypsinized, and used for preparation of HCMs in 96-well culture plates. After experimental treatments, plate wells were washed with PBS (three times), then fixed and permeabilized, and assayed according to the manufacturer's instructions (Cell Proliferation BrdU ELISA, Roche).

Imaging *C. albicans* host cell adherence

Cell monolayers in eight-well chamber slides were infected with synchronized hyphal yeast (10,000 CFU per well) by addition of a 10-μl aliquot of freshly prepared *C. albicans* inoculate to culture medium (200 μl per well) preconditioned for 36 hours with host cells. Infected slides were incubated for 2 hours, medium was removed by aspiration, and wells were washed with PBS (three times) and then fixed by 10-min incubation with 4% paraformaldehyde. Fixative was removed, and wells were washed (three times) before incubation (30 min) with Calcofluor white M2R fungal surface stain (Life Technologies) (*73*). Wells were water-washed and coverslipped before imaging by fluorescence microscopy (excitation, 360 nm/emission, 460 nm).

Immunochemical detection of *C. albicans* adhering to cell monolayers

Experiments were performed using HCMs prepared in white opaque 96-well culture plates. HCMs were infected with synchronized hyphal yeast (1000 CFU per well) by addition of 10 μl of freshly prepared *C. albicans* inoculate to wells containing preconditioned (36 hours) culture medium (100 μl per well). Wells were incubated 18 hours with yeast before aspiration of medium, gentle washing with PBS (three times), and fixation by 10-min incubation with 4% paraformaldehyde. Fixative was removed, and wells were washed (three times) before

incubation (1 hour) with blocking buffer [2% albumin in tris-buffered saline–Tween 20 (TBST)]. Wells were then incubated (2 hours) with fresh blocking buffer containing a 1:5000 dilution of α–*Candida*-HRP antibody (Abcam). Wells were washed with TBST (five times) and fluorescent-captured (excitation, 320 nm/emmision, 420 nm) after development with QuantaBlu (Pierce), a fluorescent HRP substrate.

C. albicans adhesion assay for abiotic surfaces

Experiments used a modified method of Tsai *et al.* (*22*) to assay *C. albicans* adhesion to polystyrene in conditioned culture medium. Synchronized hyphal yeast (1000 CFU per well) were incubated (37°C) in the wells of clear, flat-bottom polystyrene 96-well microtiter plates containing host cell–conditioned (36 hours) culture medium (200 μl per well). Incubation medium was removed by aspiration, and wells were washed (three times) before incubation (30 min at RT) with PBS (200 μl per well) containing 10 μl of Calcofluor white fungal stain solution 6726 (Eng Scientific). After washing, attached hyphae were detected by measuring well fluorescence (excitation, 360 nm/emmision, 460 nm).

C. albicans aggregation assay

Host cell–conditioned (48 hours) culture medium (200 μl per well) was incubated (overnight at 37°C) with synchronized yeast (200 cells per well) in the wells of clear 96-well microtiter plates. Incubation medium was removed, and yeast pellets were washed twice with PBS. During aspiration, care was taken to minimize disturbance of settled yeast at the well bottom. Settled yeast pellets were resuspended in PBS and transferred to fresh wells. Low-magnification (×4) bright-field well images were captured at maximum condenser aperture. Images were then analyzed for yeast aggregates using ImageJ software (version 1.47) with the following procedure. Captured image files were first converted from 8-bit RGB to 8-bit grayscale and then further transformed to 1-bit black and white images using a conversion threshold of 86%. Well area covered by yeast aggregates was determined from pixel counts of transformed black and white images using the Analyze Particle tool with lower size threshold set to 50 pixels. Isolated black areas of less than 50 pixels (four to six yeast cells) were not included in aggregate totals.

Staining and antibody labeling of *C. albicans* aggregates

Aggregated yeast were pelleted (2 min × 500*g*), washed with PBS (twice), and transferred to glass slides in minimal volume, and excess buffer was blotted off. Slides were air-dried to fix yeast and then carefully rinsed with water. For dye staining, slides were incubated in the dark at RT with 50 μl of Thioflavin S (5 min) or staining solution and then water-rinsed. For immunolabeling experiments, specimens prestained with Thioflavin S were incubated (2 hours at 4°C) with blocking buffer containing 1:1000 dilution of mAb 4G8. Slides were TBST-rinsed and then incubated (1 hour at RT) with donkey anti-mouse IgG antibody covalently labeled with the red fluorescent dye Alexa Fluor 594 (α–mouse-AF568) (Life Technologies). Thioflavin and anti-Aβ double-labeled specimens were mounted with Prolong Gold antifade reagent (Life Technologies) before viewing with a fluorescence confocal microscope (Leica TCS SL, Leica Microsystems).

TEM of microbial agglutinates

Candida aggregate cells suspended in PBS (5 μl) were absorbed to Formvar carbon-coated copper grids (FCF100-Cu, Electron Microscopy Sciences). Grids were blocked with 1% BSA in PBS (kept covered for 10 min at RT) and then incubated (30 min at RT) with mAb 4G8 diluted 1:1000 in blocking buffer. The grids were washed with PBS (three times) and incubated with goat anti-mouse IgG antibody covalently linked to nanogold particles. After three 5-min PBS washes and four 10-min water washes, specimens were fixed with 1% glutaraldehyde (10 min at RT). Specimens were washed with water, stained with uranyl acetate, and then viewed using a JEM-1011 transmission electron microscope (JEOL Institute).

Statistical analysis

Statistical analyses were performed with Prism software (version 6.0c). Arithmetic means were compared using two-tailed *t* tests. Survival curves were compared using log-rank (Mantel-Cox) test and confirmed by Gehan-Breslow-Wilcoxon test. *P* values <0.05 were considered statistically significant.

SUPPLEMENTARY MATERIALS

www.sciencetranslationalmedicine.org/cgi/content/full/8/340/340ra72/DC1

Materials and Methods

Fig. S1. Aβ deposition and inflammation in 5XFAD mice before infection and criteria used for assessing clinical performance after infection.

Fig. S2. Aβ42 localizes to gut and muscle in GMC101 nematodes.

Fig. S3. Aβ expression protects GMC101 nematodes and CHO-CAB cells against *S.* Typhimurium.

Fig. S4. Confirmation of increased *Candida* resistance among transformed host cells using three independent assays.

Fig. S5. Transformed cell lines generate Aβ oligomers at levels found in the soluble fraction of human brain.

Fig. S6. Transformed H4-Aβ40 and CHO-CAB host cells resist *Candida* colonization and agglutinate yeast.

Fig. S7. Birefringence of Congo red–stained yeast aggregates from H4-Aβ42 medium.

Fig. S8. Anti-Aβ antibodies do not label CL2122 tissues or yeast.

Fig. S9. β-Amyloid colocalizes with *S.* Typhimurium cells in 5XFAD brain.

Fig. S10. Model for antimicrobial activities of soluble Aβ oligomers.

Table S1. Figure micrographs are representative of data from multiple repeat experiments and image fields.

Video S1. Z-section projection of 5XFAD mouse brain showing β-amyloid entrapment of *S.* Typhimurium cells.

REFERENCES AND NOTES

1. R. E. Tanzi, L. Bertram, Twenty years of the Alzheimer's disease amyloid hypothesis: A genetic perspective. *Cell* **120**, 545–555 (2005).
2. S. Luna, D. J. Cameron, D. W. Ethell, Amyloid-β and APP deficiencies cause severe cerebrovascular defects: Important work for an old villain. *PLOS One* **8**, e75052 (2013).
3. S. J. Soscia, J. E. Kirby, K. J. Washicosky, S. M. Tucker, M. Ingelsson, B. Hyman, M. A. Burton, L. E. Goldstein, S. Duong, R. E. Tanzi, R. D. Moir, The Alzheimer's disease-associated amyloid β-protein is an antimicrobial peptide. *PLOS One* **5**, e9505 (2010).
4. B. L. Kagan, H. Jang, R. Capone, F. Teran Arce, S. Ramachandran, R. Lal, R. Nussinov, Antimicrobial properties of amyloid peptides. *Mol. Pharm.* **9**, 708–717 (2012).
5. J. Wiesner, A. Vilcinskas, Antimicrobial peptides: The ancient arm of the human immune system. *Virulence* **1**, 440–464 (2010).
6. Y. Yamaguchi, T. Nagase, T. Tomita, K. Nakamura, S. Fukuhara, T. Amano, H. Yamamoto, Y. Ide, M. Suzuki, S. Teramoto, T. Asano, K. Kangawa, N. Nakagata, Y. Ouchi, H. Kurihara, β-Defensin overexpression induces progressive muscle degeneration in mice. *Am. J. Physiol. Cell Physiol.* **292**, C2141–C2149 (2007).
7. M. Reinholz, T. Ruzicka, J. Schauber, Cathelicidin LL-37: An antimicrobial peptide with a role in inflammatory skin disease. *Ann. Dermatol.* **24**, 126–135 (2012).
8. Y. Cao, S. Chtarbanova, A. J. Petersen, B. Ganetzky, Dnr1 mutations cause neurodegeneration in *Drosophila* by activating the innate immune response in the brain. *Proc. Natl. Acad. Sci. U.S.A.* **110**, E1752–E1760 (2013).
9. A. Krause, C. Liepke, M. Meyer, K. Adermann, W. G. Forssmann, E. Maronde, Human natriuretic peptides exhibit antimicrobial activity. *Eur. J. Med. Res.* **6**, 215–218 (2001).

10. M. R. White, R. Kandel, S. Tripathi, D. Condon, L. Qi, J. Taubenberger, K. L. Hartshorn, Alzheimer's associated β-amyloid protein inhibits influenza A virus and modulates viral interactions with phagocytes. *PLOS One* **9**, e101364 (2014).
11. K. Bourgade, H. Garneau, G. Giroux, A. Y. Le Page, C. Bocti, G. Dupuis, E. H. Frost, T. Fülöp Jr., β-Amyloid peptides display protective activity against the human Alzheimer's disease-associated herpes simplex virus-1. *Biogerontology* **16**, 85–98 (2015).
12. H. Oakley, S. L. Cole, S. Logan, E. Maus, P. Shao, J. Craft, A. Guillozet-Bongaarts, M. Ohno, J. Disterhoft, L. Van Eldik, R. Berry, R. Vassar, Intraneuronal β-amyloid aggregates, neurodegeneration, and neuron loss in transgenic mice with five familial Alzheimer's disease mutations: Potential factors in amyloid plaque formation. *J. Neurosci.* **26**, 10129–10140 (2006).
13. H. Zheng, M. Jiang, M. E. Trumbauer, R. Hopkins, D. J. S. Sirinathsinghji, K. A. Stevens, M. W. Conner, H. H. Slunt, S. S. Sisodia, H. Y. Chen, L. H. T. Van der Ploeg, Mice deficient for the amyloid precursor protein gene. *Ann. N.Y. Acad. Sci.* **777**, 421–426 (1996).
14. G. McColl, B. R. Roberts, T. L. Pukala, V. B. Kenche, C. M. Roberts, C. D. Link, T. M. Ryan, C. L. Masters, K. J. Barnham, A. I. Bush, R. A. Cherny, Utility of an improved model of amyloid-beta ($A\beta_{1-42}$) toxicity in *Caenorhabditis elegans* for drug screening for Alzheimer's disease. *Mol. Neurodegener.* **7**, 57 (2012).
15. J. P. Ardizzi, H. F. Epstein, Immunochemical localization of myosin heavy chain isoforms and paramyosin in developmentally and structurally diverse muscle cell types of the nematode *Caenorhabditis elegans*. *J. Cell Biol.* **105**, 2763–2770 (1987).
16. C. I. Nussbaum-Krammer, K.-W. Park, L. Li, R. Melki, R. I. Morimoto, Spreading of a prion domain from cell-to-cell by vesicular transport in Caenorhabditis elegans. *PLOS Genet.* **9**, e1003351 (2013).
17. D. Pisa, R. Alonso, A. Rábano, I. Rodal, L. Carrasco, Different brain regions are infected with fungi in Alzheimer's disease. *Sci. Rep.* **5**, 15015 (2015).
18. R. Alonso, D. Pisa, A. I. Marina, E. Morato, A. Rábano, L. Carrasco, Fungal infection in patients with Alzheimer's disease. *J. Alzheimers Dis.* **41**, 301–311 (2014).
19. P. A. Lewis, S. Piper, M. Baker, L. Onstead, M. P. Murphy, J. Hardy, R. Wang, E. McGowan, T. E. Golde, Expression of BRI–amyloid β peptide fusion proteins: A novel method for specific high-level expression of amyloid β peptides. *Biochim. Biophys. Acta* **1537**, 58–62 (2001).
20. S. Hahn, T. Brüning, J. Ness, E. Czirr, S. Baches, H. Gijsen, C. Korth, C. U. Pietrzik, B. Bulic, S. Weggen, Presenilin-1 but not amyloid precursor protein mutations present in mouse models of Alzheimer's disease attenuate the response of cultured cells to γ-secretase modulators regardless of their potency and structure. *J. Neurochem.* **116**, 385–395 (2011).
21. C. Hock, S. Golombowski, F. Müller-Spahn, W. Naser, K. Beyreuther, U. Mönning, D. Schenk, C. Vigo-Pelfrey, A. M. Bush, R. Moir, R. Tanzi, J. H. Growdon, R. M. Nitsch, Cerebrospinal fluid levels of amyloid precursor protein and amyloid β-peptide in Alzheimer's disease and major depression—Inverse correlation with dementia severity. *Eur. Neurol.* **39**, 111–118 (1998).
22. P.-W. Tsai, C.-Y. Yang, H.-T. Chang, C.-Y. Lan, Human antimicrobial peptide LL-37 inhibits adhesion of *Candida albicans* by interacting with yeast cell-wall carbohydrates. *PLOS One* **6**, e17755 (2011).
23. A. M. Weidner, M. Housley, M. P. Murphy, H. LeVine III, Purified high molecular weight synthetic Aβ(1–42) and biological Aβ oligomers are equipotent in rapidly inducing MTT formazan exocytosis. *Neurosci. Lett.* **497**, 1–5 (2011).
24. M. P. Lambert, A. K. Barlow, B. A. Chromy, C. Edwards, R. Freed, M. Liosatos, T. E. Morgan, I. Rozovsky, B. Trommer, K. L. Viola, P. Wals, C. Zhang, C. E. Finch, G. A. Krafft, W. L. Klein, Diffusible, nonfibrillar ligands derived from $A\beta_{1-42}$ are potent central nervous system neurotoxins. *Proc. Natl. Acad. Sci. U.S.A.* **95**, 6448–6453 (1998).
25. T. Yang, S. Hong, T. O'Malley, R. A. Sperling, D. M. Walsh, D. J. Selkoe, New ELISAs with high specificity for soluble oligomers of amyloid β-protein detect natural Aβ oligomers in human brain but not CSF. *Alzheimers Dement.* **9**, 99–112 (2013).
26. R. Sood, Y. Domanov, M. Pietiäinen, V. P. Kontinen, P. K. J. Kinnunen, Binding of LL-37 to model biomembranes: Insight into target vs host cell recognition. *Biochim. Biophys. Acta* **1778**, 983–996 (2008).
27. R. Feder, A. Dagan, A. Mor, Structure-activity relationship study of antimicrobial dermaseptin S4 showing the consequences of peptide oligomerization on selective cytotoxicity. *J. Biol. Chem.* **275**, 4230–4238 (2000).
28. L. Leonova, V. N. Kokryakov, G. Aleshina, T. Hong, T. Nguyen, C. Zhao, A. J. Waring, R. I. Lehrer, Circular minidefensins and posttranslational generation of molecular diversity. *J. Leukoc. Biol.* **70**, 461–464 (2001).
29. R. I. Lehrer, Paradise lost and paradigm found. *Nat. Immunol.* **5**, 775–776 (2004).
30. N. Sal-Man, Z. Oren, Y. Shai, Preassembly of membrane-active peptides is an important factor in their selectivity toward target cells. *Biochemistry* **41**, 11921–11930 (2002).
31. D. J. Watson, A. D. Lander, D. J. Selkoe, Heparin-binding properties of the amyloidogenic peptides Aβ and amylin. Dependence on aggregation state and inhibition by Congo red. *J. Biol. Chem.* **272**, 31617–31624 (1997).
32. P.-W. Tsai, C.-Y. Yang, H.-T. Chang, C.-Y. Lan, Characterizing the role of cell-wall β-1,3-exoglucanase Xog1p in *Candida albicans* adhesion by the human antimicrobial peptide LL-37. *PLOS One* **6**, e21394 (2011).
33. J. J. Calvete, M. A. Campanero-Rhodes, M. Raida, L. Sanz, Characterisation of the conformational and quaternary structure-dependent heparin-binding region of bovine seminal plasma protein PDC-109. *FEBS Lett.* **444**, 260–264 (1999).
34. J. van Horssen, P. Wesseling, L. P. W. J. van den Heuvel, R. M. W. de Waal, M. M. Verbeek, Heparan sulphate proteoglycans in Alzheimer's disease and amyloid-related disorders. *Lancet Neurol.* **2**, 482–492 (2003).
35. M. Torrent, D. Pulido, M. V. Nogués, E. Boix, Exploring new biological functions of amyloids: Bacteria cell agglutination mediated by host protein aggregation. *PLOS Pathog.* **8**, e1003005 (2012).
36. H. Chu, M. Pazgier, G. Jung, S.-P. Nuccio, P. A. Castillo, M. F. de Jong, M. G. Winter, S. E. Winter, J. Wehkamp, B. Shen, N. H. Salzman, M. A. Underwood, R. M. Tsolis, G. M. Young, W. Lu, R. I. Lehrer, A. J. Bäumler, C. L. Bevins, Human α-defensin 6 promotes mucosal innate immunity through self-assembled peptide nanonets. *Science* **337**, 477–481 (2012).
37. K. Pütsep, G. Carlsson, H. G. Boman, M. Andersson, Deficiency of antibacterial peptides in patients with morbus Kostmann: An observation study. *Lancet* **360**, 1144–1149 (2002).
38. C. D. Ciornei, H. Tapper, A. Bjartell, N. H. Sternby, M. Bodelsson, Human antimicrobial peptide LL-37 is present in atherosclerotic plaques and induces death of vascular smooth muscle cells: A laboratory study. *BMC Cardiovas. Disord.* **6**, 49 (2006).
39. J. M. Kahlenberg, M. J. Kaplan, Little peptide, big effects: The role of LL-37 in inflammation and autoimmune disease. *J. Immunol.* **191**, 4895–4901 (2013).
40. Y. Shinkai, M. Morishima-Kawashima, Y. Ihara, M. Yoshimura, H. Shimada, Y. Ito, K. Yanagisawa, Amyloid β-protein deposition in the leptomeninges and cerebral cortex. *Ann. Neurol.* **42**, 899–908 (1997).
41. L.-O. Brandenburg, D. Varoga, N. Nicolaeva, S. L. Leib, H. Wilms, R. Podschun, C. J. Wruck, J.-M. Schröder, T. Pufe, R. Lucius, Role of glial cells in the functional expression of LL-37/rat cathelin-related antimicrobial peptide in meningitis. *J. Neuropathol. Exp. Neurol.* **67**, 1041–1054 (2008).
42. M. A. Wozniak, R. F. Itzhaki, S. J. Shipley, C. B. Dobson, Herpes simplex virus infection causes cellular β-amyloid accumulation and secretase upregulation. *Neurosci. Lett.* **429**, 95–100 (2007).
43. J. Miklossy, Chronic inflammation and amyloidogenesis in Alzheimer's disease—Role of Spirochetes. *J. Alzheimers Dis.* **13**, 381–391 (2008).
44. E. Boelen, F. R. M. Stassen, A. J. A. M. van der Ven, M. A. M. Lemmens, H. P. J. Steinbusch, C. A. Bruggeman, C. Schmitz, H. W. M. Steinbusch, Detection of amyloid beta aggregates in the brain of BALB/c mice after *Chlamydia pneumoniae* infection. *Acta Neuropathol.* **114**, 255–261 (2007).
45. C. S. Little, C. J. Hammond, A. MacIntyre, B. J. Balin, D. M. Appelt, *Chlamydia pneumoniae* induces Alzheimer-like amyloid plaques in brains of BALB/c mice. *Neurobiol. Aging* **25**, 419–429 (2004).
46. N. Papo, Y. Shai, Can we predict biological activity of antimicrobial peptides from their interactions with model phospholipid membranes? *Peptides* **24**, 1693–1703 (2003).
47. V. H. Pomin, Heparin-binding proteins (chemokines and defensins) and their complexes with glycosaminoglycans from the solution NMR perspective. *Curr. Protein Pept. Sci.* **15**, 738–744 (2014).
48. J. Wang, Y. Li, X. Wang, W. Chen, H. Sun, J. Wang, Lipopolysaccharide induces amyloid formation of antimicrobial peptide HAL-2. *Biochim. Biophys. Acta* **1838**, 2910–2918 (2014).
49. O. Goldmann, E. Medina, The expanding world of extracellular traps: Not only neutrophils but much more. *Front. Immunol.* **3**, 420 (2013).
50. S. S. Wilson, M. E. Wiens, J. G. Smith, Antiviral mechanisms of human defensins. *J. Mol. Biol.* **425**, 4965–4980 (2013).
51. P. Bergman, L. Johansson, H. Wan, A. Jones, R. L. Gallo, G. H. Gudmundsson, T. Hökfelt, A.-B. Jonsson, B. Agerberth, Induction of the antimicrobial peptide CRAMP in the blood–brain barrier and meninges after meningococcal infection. *Infect. Immun.* **74**, 6982–6991 (2006).
52. R. Bals, D. J. Weiner, A. D. Moscioni, R. L. Meegalla, J. M. Wilson, Augmentation of innate host defense by expression of a cathelicidin antimicrobial peptide. *Infect. Immun.* **67**, 6084–6089 (1999).
53. S. Eggert, K. Paliga, P. Soba, G. Evin, C. L. Masters, A. Weidemann, K. Beyreuther, The proteolytic processing of the amyloid precursor protein gene family members APLP-1 and APLP-2 involves α-, β-, γ-, and ϵ-like cleavages: Modulation of APLP-1 processing by *n*-glycosylation. *J. Biol. Chem.* **279**, 18146–18156 (2004).
54. S. A. M. Shariati, B. De Strooper, Redundancy and divergence in the amyloid precursor protein family. *FEBS Lett.* **587**, 2036–2045 (2013).
55. K. Beyreuther, P. Pollwein, G. Multhaup, U. Mönning, G. König, T. Dyrks, W. Schubert, C. L. Masters, Regulation and expression of the Alzheimer's β/A4 amyloid protein precursor in health, disease, and Down's syndrome. *Ann. N.Y. Acad. Sci.* **695**, 91–102 (1993).
56. D. Dominguez, J. Tournoy, D. Hartmann, T. Huth, K. Cryns, S. Deforce, L. Serneels, I. E. Camacho, E. Marjaux, K. Craessaerts, A. J. M. Roebroek, M. Schwake, R. D'Hooge, P. Bach, U. Kalinke, D. Moechars, C. Alzheimer, K. Reiss, P. Saftig, B. de Strooper, Phenotypic and biochemical analyses of BACE1- and BACE2-deficient mice. *J. Biol. Chem.* **280**, 30797–30806 (2005).

57. R. H. Falk, R. L. Comenzo, M. Skinner, The systemic amyloidoses. *N. Engl. J. Med.* **337**, 898–909 (1997).
58. B. L. Kagan, Antimicrobial amyloids? *Biophys. J.* **100**, 1597–1598 (2011).
59. L. Wang, Q. Liu, J.-C. Chen, Y.-X. Cui, B. Zhou, Y.-X. Chen, Y.-F. Zhao, Y.-M. Li, Antimicrobial activity of human islet amyloid polypeptides: An insight into amyloid peptides' connection with antimicrobial peptides. *Biol. Chem.* **393**, 641–646 (2012).
60. M. Pasupuleti, M. Roupe, V. Rydengård, K. Surewicz, W. K. Surewicz, A. Chalupka, M. Malmsten, O. E. Sörensen, A. Schmidtchen, Antimicrobial activity of human prion protein is mediated by its N-terminal region. *PLOS One* **4**, e7358 (2009).
61. V. Vernekar, S. Velhal, A. Bandivdekar, Evaluation of cystatin C activities against HIV. *Indian J. Med. Res.* **141**, 423–430 (2015).
62. M. Pasupuleti, M. Davoudi, M. Malmsten, A. Schmidtchen, Antimicrobial activity of a C-terminal peptide from human extracellular superoxide dismutase. *BMC Res. Notes* **2**, 136 (2009).
63. C. Shah, R. Hari-Dass, J. G. Raynes, Serum amyloid A is an innate immune opsonin for Gram-negative bacteria. *Blood* **108**, 1751–1757 (2006).
64. L. Millucci, E. Paccagnini, L. Ghezzi, G. Bernardini, D. Braconi, M. Laschi, M. Consumi, A. Spreafico, P. Tanganelli, P. Lupetti, A. Magnani, A. Santucci, Different factors affecting human ANP amyloid aggregation and their implications in congestive heart failure. *PLOS One* **6**, e21870 (2011).
65. J. Miklossy, Emerging roles of pathogens in Alzheimer disease. *Expert Rev. Mol. Med.* **13**, e30 (2011).
66. X.-L. Bu, X.-Q. Yao, S.-S. Jiao, F. Zeng, Y.-H. Liu, Y. Xiang, C.-R. Liang, Q.-H. Wang, X. Wang, H.-Y. Cao, X. Yi, B. Deng, C.-H. Liu, J. Xu, L.-L. Zhang, C.-Y. Gao, Z.-Q. Xu, M. Zhang, L. Wang, X.-L. Tan, X. Xu, H.-D. Zhou, Y.-J. Wang, A study on the association between infectious burden and Alzheimer's disease. *Eur. J. Neurol.* **22**, 1519–1525 (2015).
67. D. B. Teplow, Preparation of amyloid β-protein for structural and functional studies. *Methods Enzymol.* **413**, 20–33 (2006).
68. M. Bruatto, M. Gremmi, A. Nardacchione, M. Amerio, Effect of glucose starvation on germ-tube production by *Candida albicans*. *Mycopathologia* **123**, 105–110 (1993).
69. I. M. Stromnes, J. M. Goverman, Active induction of experimental allergic encephalomyelitis. *Nat. Protoc.* **1**, 1810–1819 (2006).
70. S. D. Miller, W. J. Karpus, Experimental autoimmune encephalomyelitis in the mouse. *Curr. Protoc. Immunol.* **Chapter 15**, 15.1.1–15.1.20 (2007).
71. S. H. Choi, K. Veeraraghavalu, O. Lazarov, S. Marler, R. M. Ransohoff, J. M. Ramirez, S. S. Sisodia, Non-cell-autonomous effects of presenilin 1 variants on enrichment-mediated hippocampal progenitor cell proliferation and differentiation. *Neuron* **59**, 568–580 (2008).
72. J. R. Powell, F. M. Ausubel, Models of *Caenorhabditis elegans* infection by bacterial and fungal pathogens. *Methods Mol. Biol.* **415**, 403–427 (2008).
73. M. J. Henry-Stanley, R. M. Garni, C. L. Wells, Adaptation of FUN-1 and Calcofluor white stains to assess the ability of viable and nonviable yeast to adhere to and be internalized by cultured mammalian cells. *J. Microbiol. Methods* **59**, 289–292 (2004).

Acknowledgments: We thank T. Golde for the Aβ-expressing transfected cell line and A. Bush for transgenic nematodes. **Funding:** This work was supported by grants from NIH (5R01AI081990-02), the Cure Alzheimer's Fund, and The Helmsley Charitable Trust. **Author contributions:** D.K.V.K., S.H.C., K.J.W., R.D.M., and R.E.T. were responsible for experimental design and data interpretation. R.D.M. and R.E.T. were responsible for manuscript preparation, with assistance from D.K.V.K., S.H.C., and K.J.W. L.E.G. and G.M. contributed to experimental design and data interpretation and developed the nematode models. W.A.E., S.T., J.G., and A.L. conducted experiments.The contributions of D.K.V.K., S.H.C., and K.J.W. overlapped extensively and included collaborations on in vitro assays, cell culture, nematode, and mouse experiments. **Competing interests:** R.D.M. is a co-inventor on a patent for the use of amyloidogenic peptides such as Aβ as possible clinical antibiotics. The other authors have no competing interests pertaining to this work.

Submitted 17 December 2015
Accepted 10 May 2016
Published 25 May 2016
10.1126/scitranslmed.aaf1059

Citation: D. K. V. Kumar, S. H. Choi, K. J. Washicosky, W. A. Eimer, S. Tucker, J. Ghofrani, A. Lefkowitz, G. McColl, L. E. Goldstein, R. E. Tanzi, R. D. Moir, Amyloid-β peptide protects against microbial infection in mouse and worm models of Alzheimer's disease. *Sci. Transl. Med.* **8**, 340ra72 (2016).

Science Translational Medicine

Amyloid-β peptide protects against microbial infection in mouse and worm models of Alzheimer's disease

Deepak Kumar Vijaya Kumar, Se Hoon Choi, Kevin J. Washicosky, William A. Eimer, Stephanie Tucker, Jessica Ghofrani, Aaron Lefkowitz, Gawain McColl, Lee E. Goldstein, Rudolph E. Tanzi and Robert D. Moir

Sci Transl Med **8**, 340ra72340ra72.
DOI: 10.1126/scitranslmed.aaf1059

Rehabilitation of a β-amyloid bad boy

A protein called Aβ is thought to cause neuronal death in Alzheimer's disease (AD). Aβ forms insoluble aggregates in the brains of patients with AD, which are a hallmark of the disease. A β and its propensity for aggregation are widely viewed as intrinsically abnormal. However, in new work, Kumar *et al*. show that Aβ is a natural antibiotic that protects the brain from infection. Most surprisingly, A β aggregates trap and imprison bacterial pathogens. It remains unclear whether A β is fighting a real or falsely perceived infection in AD. However, in any case, these findings identify inflammatory pathways as potential new drug targets for treating AD.